

Scaling laws for learning with real and surrogate data

Ayush Jain*

Andrea Montanari[†]

Eren Sasoglu*

February 8, 2024

Abstract

Collecting large quantities of high-quality data is often prohibitively expensive or impractical, and a crucial bottleneck in machine learning. One may instead augment a small set of n data points from the target distribution with data from more accessible sources like public datasets, data collected under different circumstances, or synthesized by generative models. Blurring distinctions, we refer to such data as ‘surrogate data’.

We define a simple scheme for integrating surrogate data into training and use both theoretical models and empirical studies to explore its behavior. Our main findings are: (i) Integrating surrogate data can significantly reduce the test error on the original distribution; (ii) In order to reap this benefit, it is crucial to use optimally weighted empirical risk minimization; (iii) The test error of models trained on mixtures of real and surrogate data is well described by a scaling law. This can be used to predict the optimal weighting and the gain from surrogate data.

1 Introduction and overview

1.1 Motivation and formulation

Consider a standard supervised learning setting where we are given n data points $\mathbf{z}_i = (y_i, \mathbf{x}_i)$, with covariate vectors $\mathbf{x}_i \in \mathbb{R}^d$ and response variables $y_i \in \mathbb{R}$. We would like to fit a rich parametric model $f(\cdot; \boldsymbol{\theta})$ so as to minimize the test error $R_{\text{test}}(\boldsymbol{\theta}) := \mathbb{E}L_{\text{test}}(y, f(\mathbf{x}; \boldsymbol{\theta}))$. In many application domains, the available data $\mathbf{Z} = (\mathbf{z}_i)_{i \leq n}$ from the target distribution, referred to as either *real* or *original* data, may be limited. And it may be difficult or expensive to acquire more of such data. One may then attempt to supplement these data with a different, cheaper source. Examples of such cheaper sources are (i) publicly available datasets; (ii) datasets owned by the same research group or company but acquired in different circumstances, e.g. in a different location, or using a different technology; (iii) synthetic data produced by a generative model.

We will denote the data points obtained from this source by $\mathbf{z}_i^s = (y_i^s, \mathbf{x}_i^s)$, and assume we have m of them: $\mathbf{Z}^s = (\mathbf{z}_i^s)_{i \leq m}$. We will also assume these data to have the same format as the original data, i.e., $\mathbf{x}_i^s \in \mathbb{R}^d$ and $y_i^s \in \mathbb{R}$. The distribution of these data will in general be different from the target distribution — it is commonly said that this distribution is ‘shifted.’ Therefore training on them might not be as effective as training on the original data. We will refer to \mathbf{Z}^s as ‘surrogate’ data. A number of questions arise:

1. *How should we use the surrogate data in training?*
2. *How many surrogate samples should we add to the original data?* Surrogate data still have a cost: we would like to know how to scale m with n in order to reap most of the benefits of the

*Granica Computing Inc. — granica.ai

[†]Department of Statistics and Department of Mathematics, Stanford University

added data.

3. *Does the addition of surrogate data improve test error on the original data? Can we predict this improvement?*

Our contribution is twofold:

1. We propose and study a weighted empirical risk minimization (ERM) scheme to integrate surrogate data into training.
2. We develop a scaling law to predict the test error of weighted ERM, and guide the choice of optimal weighting.

In particular, given a loss function $L : \mathbb{R} \times \mathbb{R} \rightarrow \mathbb{R}_{\geq 0}$, $(y, \hat{y}) \mapsto L(y, \hat{y})$, we consider the following regularized empirical risk:

$$\widehat{R}_{n,m}(\boldsymbol{\theta}; \alpha) := \frac{1-\alpha}{n} \sum_{i=1}^n \ell(\boldsymbol{\theta}; \mathbf{z}_i) + \frac{\alpha}{m} \sum_{i=1}^m \ell(\boldsymbol{\theta}; \mathbf{z}_i^s) + \Omega(\boldsymbol{\theta}), \quad (1)$$

where $\ell(\boldsymbol{\theta}; \mathbf{z}_i) := L(y_i, f(\mathbf{x}_i; \boldsymbol{\theta}))$, $\alpha \in [0, 1]$ is the weight of the surrogate dataset, and $\Omega : \mathbb{R}^d \rightarrow \mathbb{R}_{\geq 0}$ is a regularizer, e.g. a ridge $\Omega(\boldsymbol{\theta}) = \lambda \|\boldsymbol{\theta}\|_2^2$. We denote by

$$\widehat{\boldsymbol{\theta}}_{n,m}(\alpha) := \arg \min_{\boldsymbol{\theta}} \widehat{R}_{n,m}(\boldsymbol{\theta}; \alpha) \quad (2)$$

the corresponding empirical risk minimizer. The resulting test error will be:

$$R_{\text{test}}(\widehat{\boldsymbol{\theta}}_{n,m}(\alpha)) := \mathbb{E} L_{\text{test}}(y, f(\mathbf{x}; \widehat{\boldsymbol{\theta}}_{n,m}(\alpha))). \quad (3)$$

We allow for the test loss L_{test} to be different from the train loss L , but we will omit the subscript ‘test’ whenever clear from the context.

In words, our approach is to minimize a linear combination of the empirical risk on the original data and the empirical risk on the surrogate data. The role of the parameter α can be understood by considering the limit $m \rightarrow \infty$, where

$$\widehat{R}_{n,\infty}(\boldsymbol{\theta}; \alpha) = \frac{1-\alpha}{n} \sum_{i=1}^n \ell(\boldsymbol{\theta}; \mathbf{z}_i) + \alpha R^s(\boldsymbol{\theta}) + \Omega(\boldsymbol{\theta}),$$

and $R^s(\boldsymbol{\theta}) = \mathbb{E} \ell(\boldsymbol{\theta}; \mathbf{z}^s)$ is the population risk for surrogate data. This suggests that we can think of the surrogate data as an additional regularizer, with regularization parameter α . This leads to a simple yet important insight: adding surrogate data to the original data is typically beneficial as long as α can be chosen optimally, and m is sufficiently large, making the additional statistical noise negligible.

As a concrete example, consider the case of least squares regression, i.e., $\ell(\boldsymbol{\theta}, (y, \mathbf{x})) = (y - \langle \boldsymbol{\theta}, \mathbf{x} \rangle)^2$ and $\Omega(\boldsymbol{\theta}) = 0$. We study this case in detail in Section 5, but consider for now the special case where $m = \infty$, and the surrogate data is pure noise. Namely, y_i^s is independent of \mathbf{x}_i^s , with $\mathbb{E}\{(y_i^s)^2\} = \sigma_s^2$. Then we have

$$\widehat{R}_{n,\infty}(\boldsymbol{\theta}; \alpha) = \frac{1-\alpha}{n} \|\mathbf{y} - \mathbf{X}\boldsymbol{\theta}\|_2^2 + \alpha \|\boldsymbol{\theta}\|_{\boldsymbol{\Sigma}^s}^2 + \sigma_s^2, \quad (4)$$

where $\mathbf{y} \in \mathbb{R}^n$, $\mathbf{X} \in \mathbb{R}^{n \times d}$ is the original data, and $\boldsymbol{\Sigma}^s := \mathbb{E}\{\mathbf{x}^s (\mathbf{x}^s)^\top\}$ is the covariance matrix of the surrogate data. The equation above says that adding pure noise surrogate data is equivalent to adding a ridge penalty (more precisely, a weighted ridge, with weight determined by $\boldsymbol{\Sigma}^s$). Even

such a poor approximation of the actual data, with proper tuning of α , will generally improve the test error, especially in the noisy regime¹.

In practice, α has to be selected in a data-driven fashion, for instance by minimizing validation error. In some cases (e.g. if n is small), this can lead to inaccurate α , and hence the model trained on mixed data can underperform the one trained on original data. In alternative, one can use a theory-based choice of α , which might rely on strong modeling assumptions. Despite these caveats, we observe that the weighted ERM approach is broadly successful. Further, we find that the selection of α can be guided by a novel scaling law which we introduce and validate both theoretically and empirically in a broad range of cases.

1.2 Summary of results

We analyze the method outlined above via numerical experiments and theoretical derivations. We carry out experiments with the following data sources. (1) Simulated data from linear or Gaussian mixture models: this allows us to explicitly control the distribution shift between the original and surrogate datasets, as well as check our theoretical results in a controlled setting. (2) Real natural language processing (NLP) data for sentiment analysis, with the role of original and surrogate datasets played respectively by IMDB reviews and Rotten Tomatoes review. (3) Real image classification data, with CIFAR-10 and CIFAR-100 datasets respectively playing the role of original and surrogate data.

In addition, we carry out theoretical calculations in three different settings: (i) Classical low-dimensional asymptotics, $n \rightarrow \infty$ with d fixed (Section 3); (ii) A non-parametric function estimation setting (Section 4); (iii) High dimensional ridge regression (Section 5). For each of these cases, we study the dependence of the test error on the number of original samples n , surrogate samples m , and weight α . Our results support the following conclusions:

Leveraging surrogate data. Including surrogate data in training generally improves the test error on the original data, even if the surrogate data distribution is very far from the original one. In agreement with the interpretation of surrogate data as a regularizer (as exemplified by the model (4)) the improvement is significant when either the original dataset size is small, or the surrogate data distribution is close to the original one.

Tuning of α . The above conclusion holds under the condition that α can be tuned (nearly) optimally. For each of the theoretical settings already mentioned, we characterize this optimal value. The general behavior matches intuition in each of these cases: α should be closer to one when either the original dataset is small, or the surrogate data distribution is close to the original one. We verify that nearly optimal α can be selected by minimizing error on a validation split of the original data. An attractive alternative is to use the scaling law we discuss next.

Scaling law. We propose a general scaling law that captures the behavior of the test error with m, n, α :

$$R(\hat{\theta}_{m,n}(\alpha)) - R_* \approx \alpha^2 R_{\text{su}}^{\text{ex}}(\infty) + [\alpha^2 (R_{\text{su}}^{\text{ex}}(m) - R_{\text{su}}^{\text{ex}}(\infty))^{1/\beta} + (1 - \alpha)^2 R_{\text{or}}^{\text{ex}}(n)^{1/\beta}]^\beta. \quad (5)$$

Here R_* is the minimal (Bayes) error, $R_{\text{su}}^{\text{ex}}(m) := R(\hat{\theta}_{m,0}(1)) - R_*$ is the excess test error when training on the surrogate data (and testing on original), $R_{\text{or}}^{\text{ex}}(n) := R(\hat{\theta}_{0,n}(0)) - R_*$ is the excess test error² when training on original data (and testing on original), and β is a scaling exponent. (The above scaling admits natural generalizations, which we discuss in Section 6.)

¹But not if the original data is noiseless and $n > d$.

²We assume here that $R_{\text{or}}^{\text{ex}}(\infty) = 0$, i.e. that we achieve Bayes risk with infinitely many original samples. See Section 6.

This scaling law captures the theoretical results of Section 3 to 5, and we check that it describes well the behavior of test error in a variety of empirical settings.

Scaling laws have been broadly successful in guiding the development of large machine learning models [HNA⁺17, RRBS19, HKK⁺20, KMH⁺20, TDR⁺21, HKHM21, HBM⁺22, ANZ22, MRB⁺23]. We expect them to be similarly useful in integrating heterogeneous data into training.

From a practical perspective, given data $\{z_i\}_{i \leq n}$ and a source of surrogate data, we would like to predict how much the test error can be decreased by including any number m of surrogate samples to the mix. The scaling law (5) suggests a simple approach:

1. Learn models on purely original data to extract the behavior of test loss $R(\hat{\theta}_{0,n}(0))$.
2. Learn models on purely surrogate data to extract the behavior of $R(\hat{\theta}_{m,0}(1))$.
3. Use the minimum over α of Eq. (5) to predict test error at any given pair m, n .

1.3 Related work

The use of a mixture of real and surrogate data to enhance training has attracted significant research effort in recent years. The interest in these topics has grown over time, because of the recent progresses in generative modeling.

This line of work has largely focused on the techniques to generate synthetic data that are well suited for training. A broad variety of methods have been demonstrated to be useful to generate data for computer vision tasks, ranging from object classification to semantic segmentation [RSM⁺16, JRBM⁺17, AAMM⁺18, TPA⁺18, CLCG19, HSY⁺22, MPT⁺22, YCFB⁺22]. We refer to [SLW20] for a review. More recently, synthetic data have been used for training in natural language processing [HNK⁺22, MHZH22].

The change of scaling laws when training on synthetic data was the object of a recent empirical study [FCK⁺23]. The approach proved successful, although scaling exponents appear to deteriorate. On the other hand, no systematic attempt was made at integrating real and synthetic data.

Our results are also relevant to problems in transfer learning. However, that literature focuses on learning shared data representations rather than training a unique model for the target distribution [MPRP16, TJJ20].

2 Empirical results

In this section, we present experiments on a variety of datasets, providing evidence for the scaling law (5).

The datasets we use include both simulated and real-world data. For simulated data, we select two different distributions for the original and surrogate datasets. The test and validation sets are generated from the same distribution as the original dataset. In case of real-world data, we choose two different datasets as the original and surrogate datasets. We divide the original dataset into train, test, and validation sets, while all examples in the surrogate datasets are allocated solely to the train split. For each experiment run, we randomly draw examples from the train split of both the original and surrogate datasets.

We report excess prediction risk (under square loss) for regression examples, and test classification error for classification examples.

For each dataset and model discussed in this section, we carry out the same experiment: (i) We use models trained on original data to fit the scaling curve $R(\hat{\theta}_{0,n}(0)) = A_{or} + B_{or}n^{-\beta_{or}}$ and obtain A_{or} and β_{or} (ii) We use models trained on purely surrogate data to fit the scaling curve $R(\hat{\theta}_{m,0}(1)) =$

$A_{\text{su}} + B_{\text{su}}m^{-\beta_{\text{su}}}$ to obtain A_{su} and β_{su} . (iii) Since we have assumed $R_* = R(\hat{\theta}_{0,\infty}(0))$, we let $R_* = A_{\text{or}}$ and excess risk estimates $R_{\text{or}}^{\text{ex}}(n) = R(\hat{\theta}_{0,n}(0)) - A_{\text{or}}$, $R_{\text{su}}^{\text{ex}}(m) = R(\hat{\theta}_{m,0}(1)) - A_{\text{or}}$ and $R_{\text{su}}^{\text{ex}}(\infty) = A_{\text{su}} - A_{\text{or}}$, and we use $\beta = \beta_{\text{or}}$, the fit exponent obtained from original data); (iv) For each combination of m, n , we use our estimates of $R_{\text{su}}^{\text{ex}}(m)$, $R_{\text{or}}^{\text{ex}}(n)$ (as measured empirically on the test set), β , $R_{\text{su}}^{\text{ex}}(\infty)$, and R_* to plot the predicted $R(\theta_{m,n}(\alpha))$ as a function of α using scaling law (5). (v) We then train the model using n original and m surrogate examples with weights $(1 - \alpha)$ and α for the two datasets, respectively. We average the results of multiple independent runs to compare it against those predicted by the scaling law. For ridge regression, we also compare with exact high-dimensional asymptotics.

2.1 Binary classification with Gaussian mixture data

This is a simple simulated setting. The original dataset consists of independent and identically distributed examples $(y_i, \mathbf{x}_i) \in \mathbb{R} \times \mathbb{R}^d$, $d = 200$, where y_i is uniform over $\{+1, -1\}$, and $\mathbf{x}_i|_{y_i} \sim \mathcal{N}(y_i\theta_*, \mathbf{I}_d)$, where $\theta_* \in \mathbb{R}^d$, $\|\theta_*\| = 1$. Surrogate data have the same distribution, with a different unit vector $\theta_{*,s}$. This data distribution is parametrized by d and the angle γ between the original and surrogate parameters, $\cos \gamma := \langle \theta_*, \hat{\theta}_{*,s} \rangle$. We use $\gamma = \pi/10$ in our experiments. For each (m, n, α) , we average the results over 10 independent runs.

We use two different models for classification: (1) Logistic regression; (2) A one-hidden layer neural network with 32 hidden ReLU neurons.

Results for logistic regression are presented in appendix. For the neural network model, they are shown in Figures 1 and 2. In this as well as (most of) the examples in next subsections, we observe that the scaling law captures well the behavior of the test error for data mixtures.

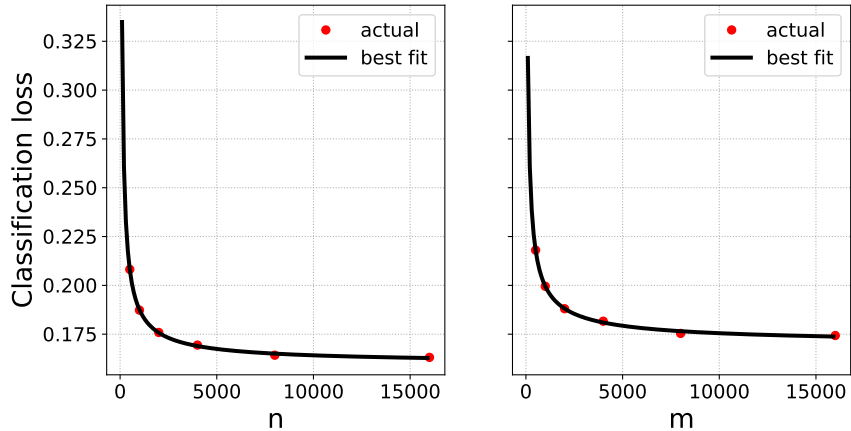


Figure 1: Gaussian mixture data and neural network. Test error scaling of the original data (left), and surrogate data (right). Best curve fits give the estimates exponent $\beta = 0.79$, $R_* = 0.160$ and $R_{\text{su}}^{\text{ex}}(\infty) = 0.010$.

2.2 Sentiment analysis in movie reviews

As original data, we use the IMDB dataset (huggingface.co/datasets/imdb) which has 25k reviews for training, each labeled as positive or negative. As surrogate data, we use the Rotten

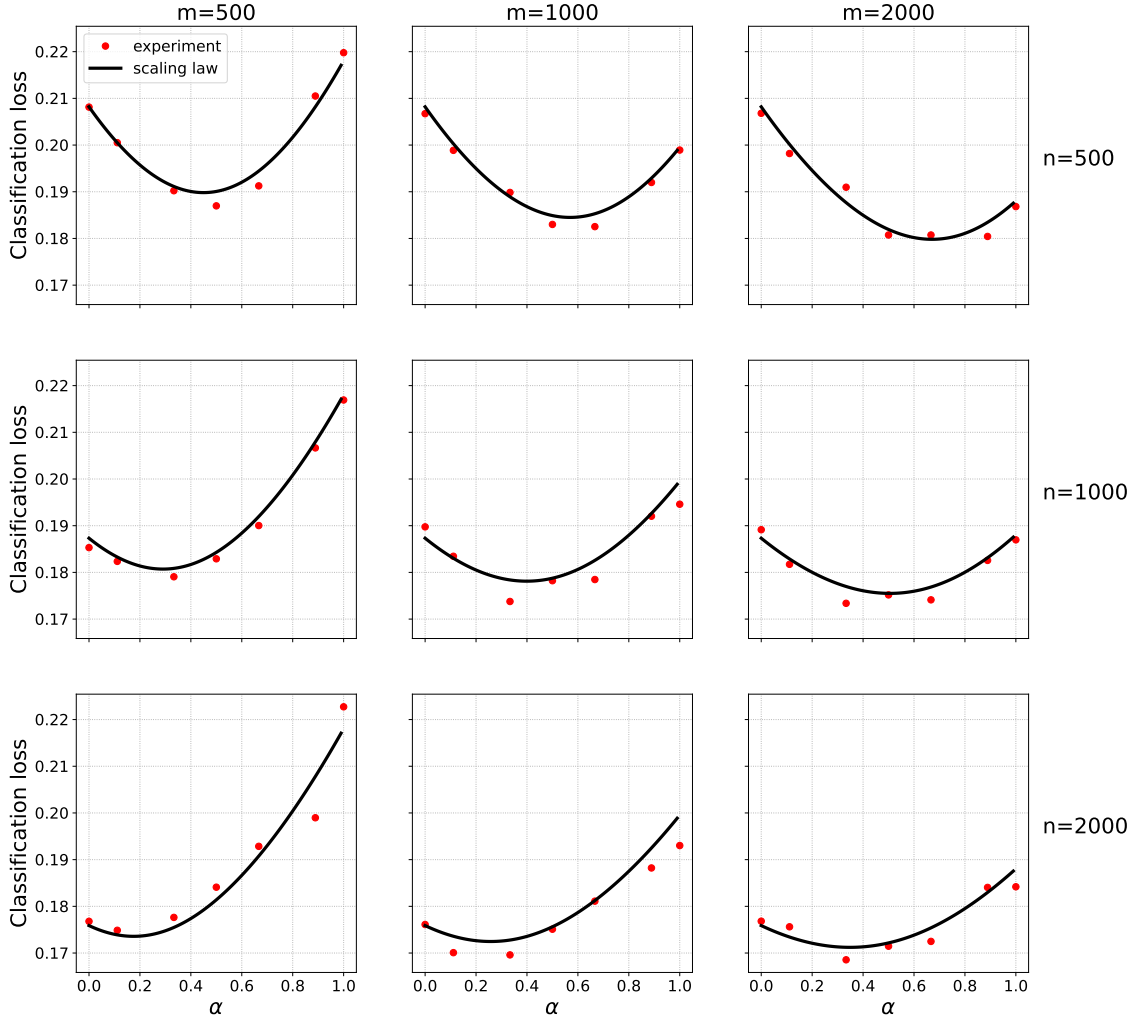


Figure 2: Gaussian mixture data and neural network. Test error when training mixture of original (n varying by row) and surrogate (m varying by column) data. Black curves: scaling law (5).

Tomatoes dataset (huggingface.co/datasets/rotten_tomatoes), combining the training, test, and validation sets into a single training set of 10.67k reviews, which are labeled similarly. For validation and testing, we split the IMDB test dataset of 25k reviews into a validation set of 10k reviews and test set of 15k reviews.

We convert reviews into feature vectors with $d = 884$ dimensions as explained in Appendix A.2. We use logistic regression and neural network models with the same set of parameters as in the Gaussian mixture experiments (except for the input dimension).

Results with neural nets are presented in Figure 3 (see appendix for further results).

2.3 Image classification with CIFAR10 and CIFAR100

We use 50,000 CIFAR10 training images as original data, its 10 classes for the classification task, and test on the 10,000 CIFAR10 test images. We use 50,000 CIFAR100 training images as surrogate data. We train a 9-layer ResNet model for classification. Appendix A.3 presents details on the data pre-processing and mapping of labels.

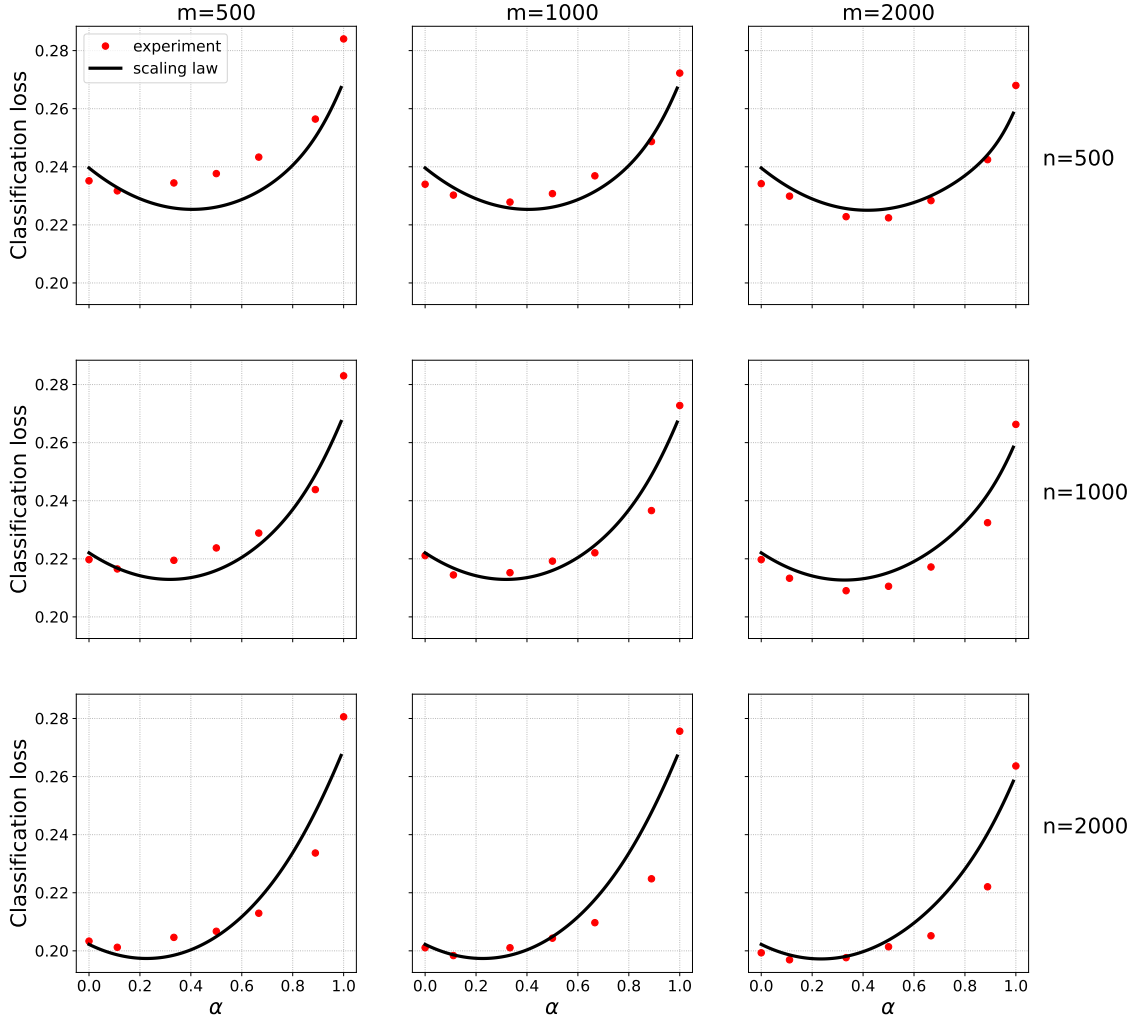


Figure 3: IMDB and Rotten Tomatoes data and neural networks. Test error when trained on mixtures of original and surrogate data. Black curves: prediction from Eq. (5).

Results are shown in Figure 4.

2.4 High-dimensional ridge regression

We finally consider simulated data distributed according to a simple linear model $y_i = \langle \boldsymbol{\theta}_*, \mathbf{x}_i \rangle + \varepsilon_i$, $i \leq n$; $y_i^s = \langle \boldsymbol{\theta}_{*,s}, \mathbf{x}_i^s \rangle + \varepsilon_i^s$, $i \leq m$; with $\mathbf{x}_i, \mathbf{x}_i^s \sim \mathbf{N}(\mathbf{0}, \mathbf{I}_d)$, $\varepsilon_i \sim \mathbf{N}(0, \sigma^2)$, $\varepsilon_i^s \sim \mathbf{N}(0, \sigma_s^2)$. We fit a simple linear model using ridge regression (see also Section 5). In our experiments for Figure 5, we use $d = 500$, $\sigma^2 = \sigma_s^2 = 1$, $\|\boldsymbol{\theta}_*\| = \|\boldsymbol{\theta}_{*,s}\| = 1$ and regularization parameter $\lambda = 2^{-10}$. Under these settings, the model is parametrized by the angle γ between $\boldsymbol{\theta}_*$ and $\boldsymbol{\theta}_{*,s}$, where $\cos \gamma := \langle \boldsymbol{\theta}_*, \boldsymbol{\theta}_{*,s} \rangle$. We used $\gamma = \pi/6$ and $\pi/2$ in our experiments.³

In Section 5, we present a theoretical prediction for these curves in the high-dimensional asymptotics $m, n, d \rightarrow \infty$, with $n/d \rightarrow \delta$, $m/d \rightarrow \delta_s$ (see Proposition 2). These theoretical predictions are reported as blue lines in these figures, and match remarkably well with the empirical data.

³For ridge regression simulations, we directly plot the excess test risks, as the parameter $\boldsymbol{\theta}$ for original data is known. For any $\hat{\boldsymbol{\theta}}$ the excess test risk in this model is simply $\|\boldsymbol{\theta} - \hat{\boldsymbol{\theta}}\|^2$.

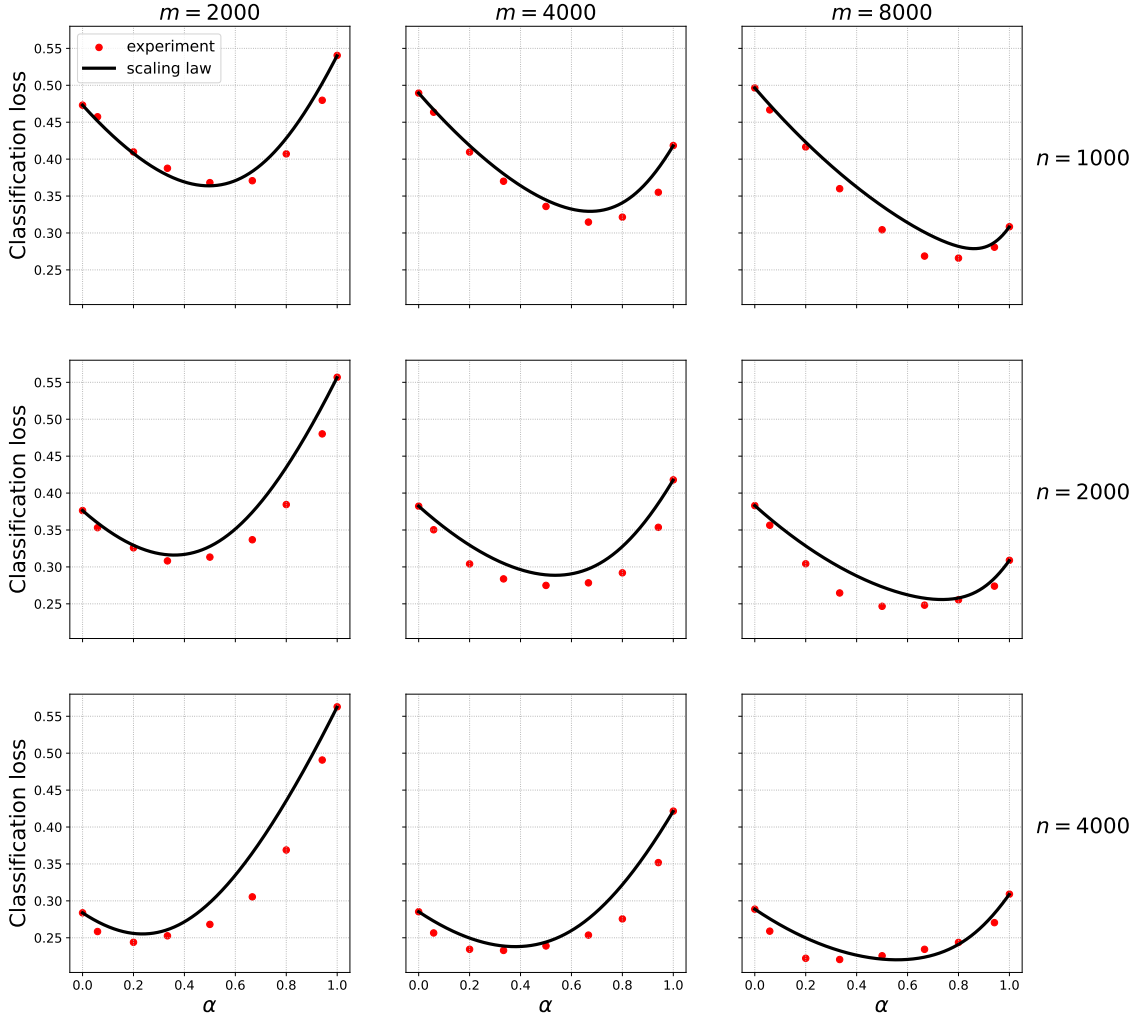


Figure 4: CIFAR10 and CIFAR100 data. Test error when trained on mixtures of original and surrogate data. Black curves: prediction from Eq. (5).

The simple scaling law (5) nevertheless provides a good approximation of these (more complicated) theoretical formulas.

Note in particular that in the top row of Figure 5, we have $\langle \theta_*, \theta_{*,s} \rangle = 0$, i.e. the surrogate data are as far as possible from the original ones. Nevertheless, the induced regularization effect leads to smaller test error on the original distribution.

2.5 Discussion

We observe the following in all of the datasets above, and for most combinations of original and surrogate examples we have tested.

1. The proposed scaling law (5) predicts well the behavior of the experiments, across a range of m and n : both the optimal value of α and the optimal gain in test error are captured quite well by our approach.
2. Adding surrogate data improves test error, provided that it is weighted optimally or near

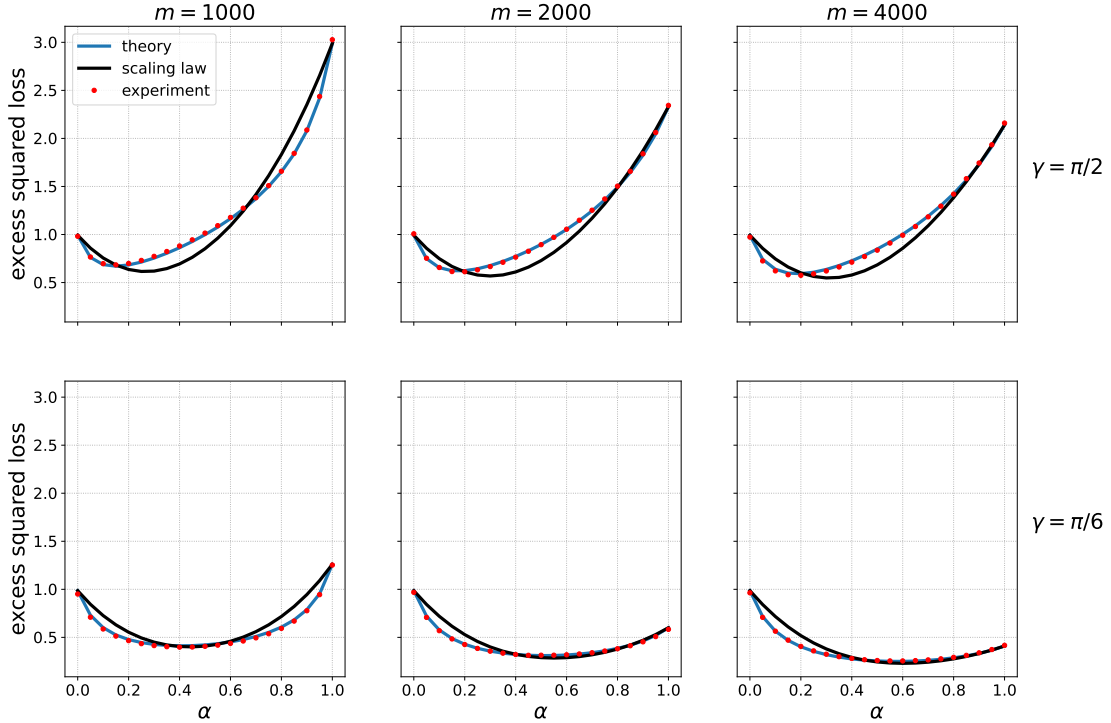


Figure 5: Ridge regression on simulated data. Here $d = 500$, $n = 1000$, $\sigma^2 = \sigma_s^2 = 1$, $\|\boldsymbol{\theta}_*\| = \|\boldsymbol{\theta}_{*,s}\| = 1$, regularization parameter $\lambda = 2^{-10}$, and m varies by column. Top row $\gamma = \pi/2$, bottom row $\gamma = \pi/6$.

optimally. That is, the test risk with the optimal choice of α is typically lower than the test risk with $\alpha = 0$.

3. For fixed original dataset size n , the optimal weight for surrogate data increases with m . This is not surprising, since test error improves with size when trained only on surrogate data, and therefore all else being equal, larger surrogate datasets must be given more weight. The same conclusion holds for fixed m and increasing n .
4. The improvement over $\alpha = 0$ decreases with n . This is also natural, since in the limit $n = \infty$, no amount of surrogate data will help.
5. Also matching intuition, the improvement in test error due to surrogate data is larger, when the surrogate data distribution is closer to the original data distribution, as demonstrated in Fig. 5 for the case of ridge regression.

Finally, we emphasize that the scaling law is only an empirical approximation of reality. This is clearly illustrated by the example of ridge regression. *First*, Fig. 5 shows a small but non-vanishing discrepancy between the scaling law prediction, and the asymptotically exact prediction derived in Section 5. *Second*, in the appendix we present simulated examples (within the same ridge regression model) in which the prediction of Eq. (5) fails significantly. On the other hand, these failures are not unexpected, as they concern cases in which even standard scaling (at $\alpha = 0$ or $\alpha = 1$) fails.

3 Low-dimensional asymptotics

As a first attempt at a theoretical explanation, we consider the estimator of Eqs. (1), (2) under the classical asymptotics $m, n \rightarrow \infty$ at d fixed. For simplicity, we assume no regularizer is used in this regime.

Beyond classical regularity assumptions of low-dimensional asymptotics, in this section we will make the following assumption which guarantees that original and surrogate distribution are ‘not arbitrarily far.’ (Recall that $R^s(\boldsymbol{\theta})$ denotes the population error on surrogate data.)

Assumption 1 (Distribution shift for low- d asymptotics). *There exists a constant K_* such that for all $\boldsymbol{\theta} \in \mathbb{R}^d$,*

$$|R^s(\boldsymbol{\theta}) - R(\boldsymbol{\theta})| \leq K_*(1 + R(\boldsymbol{\theta})). \quad (6)$$

The regularity conditions are similar to the ones in [vdV00] and collected as Assumption 2 (Appendix B.)

Proposition 3.1. *Under Assumption 1 and Assumption 2, define the following $d \times d$ matrices*

$$\mathbf{H} := \nabla^2 R(\boldsymbol{\theta}_*) = \mathbb{E}[\nabla^2 \ell(\boldsymbol{\theta}_*; \mathbf{z})], \quad (7)$$

$$\mathbf{K} := \text{Cov}(\nabla \ell(\boldsymbol{\theta}_*; \mathbf{z}); \nabla \ell(\boldsymbol{\theta}_*; \mathbf{z})), \quad (8)$$

$$\mathbf{K}_s := \text{Cov}_s(\nabla \ell(\boldsymbol{\theta}_*; \mathbf{z}^s); \nabla \ell(\boldsymbol{\theta}_*; \mathbf{z}^s)), \quad (9)$$

where Cov , Cov_s denote the covariances, respectively, with respect to the original data (i.e., with respect to $\mathbf{z} \sim \mathbb{P}$), and with respect to the surrogate data (i.e., with respect to $\mathbf{z}^s \sim \mathbb{P}_s$). Further define the d -dimensional vector

$$\mathbf{g}^s := \nabla R^s(\boldsymbol{\theta}_*) - \nabla R(\boldsymbol{\theta}_*). \quad (10)$$

Then there exists $\alpha_{\max} \in (0, 1]$ (depending only on the constants in the assumptions) such that, for all $\alpha \in [0, \alpha_{\max}]$, the excess risk of the estimator $\hat{\boldsymbol{\theta}}_{m,n}(\alpha)$ satisfies (for $D := \|\mathbf{g}^s\|$ bounded by a constant)

$$\begin{aligned} R(\hat{\boldsymbol{\theta}}_{m,n}(\alpha)) - R(\boldsymbol{\theta}_*) &= \alpha^2 \langle \mathbf{g}^s, \mathbf{H}^{-1} \mathbf{g}^s \rangle + \frac{(1 - \alpha)^2}{n} \cdot \text{Tr}(\mathbf{H}^{-1} \mathbf{K}) \\ &+ \frac{\alpha^2}{m} \cdot \text{Tr}(\mathbf{H}^{-1} \mathbf{K}_s) + O\left(\left(\frac{1}{m \vee n} + D\alpha^2\right)\left(\frac{1}{(m \vee n)^{1/2}} + D\alpha\right)\right). \end{aligned} \quad (11)$$

(Here the big O hides dependence on the constants in Assumptions 1 and 2.)

Remark 3.1. For economy of notation we stated Proposition 3.1 in the case in which the excess risk is measured by using the same loss as for training, i.e. $\ell_{\text{test}} = \ell$. However the same result Eq. (11) applies with minor modifications to the case $\ell_{\text{test}} \neq \ell$ (and thus, with R replaced by R^{test}), provided R^{test} is also twice differentiable with Lipschitz Hessian, and $\nabla R^{\text{test}}(\boldsymbol{\theta}_*) = \mathbf{0}$. In this case, (11) has to be modified replacing \mathbf{H}^{-1} by $\mathbf{H}^{-1} \nabla^2 R^{\text{test}}(\boldsymbol{\theta}_*) \mathbf{H}^{-1}$.

Remark 3.2. The error terms in Eq. (11) are negligible under two conditions: (i) m and n are large, which is the classical condition for low-dimensional asymptotics to hold; (ii) $\|\mathbf{g}^s\|_2 = \|\nabla R^s(\boldsymbol{\theta}_*)\|_2 \alpha$ is small. In particular, the latter condition will hold in two cases. *First*, when $\|\nabla R^s(\boldsymbol{\theta}_*)\|_2$ is of order one (i.e. the distribution shift is large), but α is small (surrogate data are downweighted).

Note that, when the distribution shift is large, and the sample size n is large enough, we expect small α to be optimal and therefore Eq. (11) covers the ‘interesting’ regime.

Second, when $\|\nabla R^s(\boldsymbol{\theta}_*)\|_2$ is small (i.e. the shift is small) and α is of order one. If in addition we have $\nabla^2 R^s(\boldsymbol{\theta}_*) \approx \nabla^2 R^s(\boldsymbol{\theta}_*)$, it can be shown that the range of validity of Eq. (11) covers the whole interval $\alpha \in [0, 1]$.

Remark 3.3. Note that the distribution shift is measured in Eq. (11) by the first term $\langle \mathbf{g}^s, \mathbf{H}^{-1} \mathbf{g}^s \rangle$. The original and surrogate distribution can be very different in other metrics (e.g. in total variation or transportation distance), but as long as \mathbf{g}^s is small (as measured in the norm defined by \mathbf{H}^{-1}), surrogate data will reduce test error.

Note that, within the setting of Proposition 3.1, the excess error of training only on original data is $R_{\text{or}}^{\text{ex}}(n) := R(\hat{\boldsymbol{\theta}}_{0,n}(0)) - R(\boldsymbol{\theta}_*) = \text{Tr}(\mathbf{H}^{-1} \mathbf{K})/n + o(1/n)$, while $R_{\text{su}}^{\text{ex}}(m) := R(\hat{\boldsymbol{\theta}}_{m,n}(0)) - R(\boldsymbol{\theta}_*) = \langle \mathbf{g}^s, \mathbf{H}^{-1} \mathbf{g}^s \rangle + \text{Tr}(\mathbf{H}^{-1} \mathbf{K}_s)/m + o(1/m)$. Hence Eq. (3.1) can be recast in the form of our general scaling law (5), namely:

$$R(\hat{\boldsymbol{\theta}}_{m,n}(\alpha)) - R(\boldsymbol{\theta}_*) \approx \alpha^2 R_{\text{su}}^{\text{ex}}(\infty) + \left[\alpha^2 (R_{\text{su}}^{\text{ex}}(m) - R_{\text{su}}^{\text{ex}}(\infty)) + (1 - \alpha)^2 R_{\text{or}}^{\text{ex}}(n) \right],$$

which (as expected) corresponds to the parametric scaling exponent $\beta = 1$.

An immediate consequence of Proposition 3.1 is that surrogate data do not hurt, and will help if their distribution is close enough to the original one (under the assumption of optimally chosen α).

Corollary 3.2. *Under the assumptions of Proposition 3.1, let $\bar{R}_{\text{or}}(n) := \text{Tr}(\mathbf{H}^{-1} \mathbf{K})/n$, and $\bar{R}_{\text{su}}(m) := \langle \mathbf{g}^s, \mathbf{H}^{-1} \mathbf{g}^s \rangle + \text{Tr}(\mathbf{H}^{-1} \mathbf{K}_s)/m$. For $\alpha_{m,n}^* = \bar{R}_{\text{or}}(n)/(\bar{R}_{\text{su}}(m) + \bar{R}_{\text{or}}(n))$, we have*

$$R(\hat{\boldsymbol{\theta}}_{m,n}(\alpha_{m,n}^*)) - R_* = (\bar{R}_{\text{or}}(n)^{-1} + \bar{R}_{\text{su}}(m)^{-1})^{-1} + \Delta_{m,n},$$

with $\Delta_{m,n}$ of the same order as the error in Prop. 3.1.

4 A non-parametric model

In this section we consider the classic non-parametric regression model. We assume that $n = Q^d$ for some integer $Q \geq 2$, and the original data $(\mathbf{x}_i, y_i)_{i \leq n}$ are defined through

$$y_i = f_*(\mathbf{x}_i) + \varepsilon_i, \quad \varepsilon_i \sim \mathbf{N}(0, \sigma^2), \quad (12)$$

where ε_i are independent of \mathbf{x}_i and of each other, and $\{\mathbf{x}_i\}_{i \leq n}$ equally spaced grid points in the d -dimensional unit-cube, i.e. $\mathcal{X}_n = \{\mathbf{q}/Q : \mathbf{q} \in [Q]^d\}$. Surrogate data have a similar distribution, with $m = Q_s^d$ equally spaced points \mathbf{x}_i^s in the unit cube, and $y_i^s = f_{*,s}(\mathbf{x}_i^s) + \varepsilon_i^s$, where $\varepsilon_i^s \sim \mathbf{N}(0, \sigma_s^2)$. We assume that f_* has small Sobolev norm, that is,

$$\|f_*\|_{r,2}^2 := \int_{[0,1]^d} (|f_*(t)|^2 + \|f_*^{(r)}(t)\|^2) dt \leq 1.$$

Recall that $\|f\|_{r,2}^2$ is a special reproducing kernel Hilbert space (RKHS) norm: we expect some of the considerations below to generalize to other RKHS norms.

Following our general methodology, we minimize a combination on the empirical risk on surrogate and original data

$$\hat{f}_{m,n,\alpha} = \arg \min_f \left\{ \frac{1-\alpha}{n} \sum_{i=1}^n (y_i - f(\mathbf{x}_i))^2 + \frac{\alpha}{m} \sum_{i=1}^m (y_i^s - f(\mathbf{x}_i^s))^2 + \lambda \|f\|_{p,2}^2 \right\}. \quad (13)$$

We are interested in $R(f) = \mathbb{E}\{(f(\mathbf{x}) - f_*(\mathbf{x}))^2\}$, which is the excess squared loss for a test point $\mathbf{x} \sim \text{Unif}([0, 1]^d)$.

In order to avoid technical burden we will carry out the analysis for a continuous model, the so-called white noise model, where we observe the function f at all points $\mathbf{x} \in [0, 1]^d$, perturbed by d -dimensional white noise:

$$dY = f_*(\mathbf{x}) d\mathbf{x} + \frac{\sigma}{\sqrt{n}} dB(\mathbf{x}), \quad (14)$$

and similarly for Y^s . We use an estimator that naturally generalizes (13) to the continuous case:

$$\hat{f}_{m,n,\alpha} = \arg \min_f \left\{ (1 - \alpha) \|Y - f\|_2^2 + \alpha \|Y^s - f\|_2^2 + \lambda \|f\|_{p,2}^2 \right\}. \quad (15)$$

Remark 4.1. The white noise model (14) is known to be equivalent to the original model (12) (with deterministic equispaced designs) in the sense of Le Cam, for $r > d/2$ [BL96, Rei08]. While suggestive, this equivalence does not allow us to formally deduce results for the data (12), because it does not apply to the specific estimators of interest here.

Our analysis for this model is analogous of textbook results in nonparametric statistics [Tsy09].

Theorem 1. *Let $\beta = (2p \wedge 4r)/(d + (2p \wedge 4r))$. If $r > d/4$ and $\lambda = (\delta K_{n,m} \sigma^2)^{2r/(d+(2p \wedge 4r))}$, then for every $\delta \in (0, 1)$ there exists a constant $C = C(d, \delta)$ such that*

$$R(\hat{f}_{m,n,\alpha}) \leq (1 + \delta) \alpha^2 R_{\text{su}}^{\text{ex}}(\infty) + C \left\{ (1 - \alpha)^2 \cdot \frac{\sigma^2}{n} + \alpha^2 \cdot \frac{\sigma_s^2}{m} \right\}^\beta \quad (16)$$

with high probability, where $K_{n,m} := (1 - \alpha)^2/n + \alpha^2/m$.

Remark 4.2. With the given choice of λ , r , the derivation of (16) also implies $R_{\text{su}}^{\text{ex}}(m) - R_{\text{su}}^{\text{ex}}(\infty) \geq C'(\sigma_s^2/m)^\beta$, $R_{\text{or}}^{\text{ex}}(n) \geq C'(\sigma/n)^\beta$ (for the least favorable f [Tsy09]). Therefore (16) is consistent with the scaling law (5) (although it falls short of proving it).

5 High-dimensional linear regression

In this section, we study ridge regression in the high-dimensional regime in which the number of samples is proportional to the number of parameters. Denoting the original data by (\mathbf{y}, \mathbf{X}) (with $\mathbf{y} \in \mathbb{R}^n$ the vector of responses and $\mathbf{X} \in \mathbb{R}^{n \times d}$ the matrix of covariates), and the surrogate data by $(\mathbf{y}^s, \mathbf{X}^s)$ (with $\mathbf{y}^s \in \mathbb{R}^m$ and $\mathbf{X}^s \in \mathbb{R}^{m \times d}$), we minimize the regularized empirical risk

$$\hat{R}_{n,m}(\boldsymbol{\theta}; \alpha) = \frac{1 - \alpha}{2n} \|\mathbf{y} - \mathbf{X}\boldsymbol{\theta}\|_2^2 + \frac{\alpha}{2m} \|\mathbf{y}^s - \mathbf{X}^s\boldsymbol{\theta}\|_2^2 + \frac{\lambda}{2} \|\boldsymbol{\theta}\|_2^2, \quad (17)$$

We assume a simple distribution, whereby the rows of \mathbf{X} , \mathbf{X}^s (denoted by \mathbf{x}_i , \mathbf{x}_i^s) are standard normal vectors and

$$\mathbf{y} = \mathbf{X}\boldsymbol{\theta}_* + \boldsymbol{\varepsilon}, \quad \mathbf{y}^s = \mathbf{X}^s\boldsymbol{\theta}_*^s + \boldsymbol{\varepsilon}^s. \quad (18)$$

for $\boldsymbol{\varepsilon} \sim \mathbf{N}(\mathbf{0}, \sigma^2 \mathbf{I}_n)$, $\boldsymbol{\varepsilon}^s \sim \mathbf{N}(\mathbf{0}, \sigma_s^2 \mathbf{I}_m)$. Note that the two data distributions differ in the true coefficient vectors $\boldsymbol{\theta}_*$ versus $\boldsymbol{\theta}_{*,s}$ as well as in the noise variance. We will denote by $\hat{\boldsymbol{\theta}}_{n,m}(\alpha)$ the ridge estimator, i.e.

$$\hat{\boldsymbol{\theta}}_{n,m}(\alpha) = \arg \min_{\boldsymbol{\theta} \in \mathbb{R}^d} \hat{R}_{n,m}(\boldsymbol{\theta}; \alpha). \quad (19)$$

The excess test error (for square loss) is given by $R(\hat{\boldsymbol{\theta}}) := \mathbb{E}\{(\langle \mathbf{x}, \boldsymbol{\theta}_* \rangle - \langle \mathbf{x}, \hat{\boldsymbol{\theta}} \rangle)^2\} = \|\hat{\boldsymbol{\theta}} - \boldsymbol{\theta}_*\|^2$. The next result characterizes this error in the proportional asymptotics, $n, m, d \rightarrow \infty$ with $n/d \rightarrow \delta$, $m/d \rightarrow \delta_s$.

Our characterization is given in terms of a variational principle. For $\delta, \delta_s \in (0, \infty)$, define $\mathcal{R} : \mathbb{R}_{\geq 0}^3 \rightarrow \mathbb{R}$ via

$$\begin{aligned} \mathcal{R}(\xi, \xi_{\perp}, \omega) &:= -\omega\sqrt{\rho^2 + \rho_s^2} + \rho\sqrt{\delta(\tau^2 + \sigma^2)} + \rho_s\sqrt{\delta_s(\tau_s^2 + \sigma_s^2)} - \frac{\delta\rho^2}{2(1-\alpha)} \\ &\quad - \frac{\delta_s\rho_s^2}{2\alpha} + \frac{\lambda}{2}(\xi^2 + \xi_{\perp}^2 + \omega^2), \end{aligned} \quad (20)$$

where τ, τ_s are defined by

$$\tau^2 := (\xi - r)^2 + \xi_{\perp}^2 + \omega^2, \quad (21)$$

$$\tau_s^2 := (\xi - r_s \cos \gamma)^2 + (\xi_{\perp} - r_s \sin \gamma)^2 + \omega^2, \quad (22)$$

and $\rho = \bar{\rho}/\sqrt{1+t^2}$, $\rho_s = \bar{\rho}t/\sqrt{1+t^2}$, with $\bar{\rho}$ solving the polynomial equation

$$\bar{\rho}^2 = \frac{\delta(\tau^2 + \sigma^2)}{(\delta/(1-\alpha) + \omega/\bar{\rho})^2} + \frac{\delta_s(\tau_s^2 + \sigma_s^2)}{(\delta_s/\alpha + \omega/\bar{\rho})^2}, \quad (23)$$

and t is given by

$$t = \frac{\omega + \delta\bar{\rho}/(1-\alpha)}{\omega + \delta_s\bar{\rho}/\alpha} \cdot \sqrt{\frac{\delta_s(\tau_s^2 + \sigma_s^2)}{\delta(\tau^2 + \sigma^2)}}. \quad (24)$$

The asymptotics of the test error is determined by the minimizer of \mathcal{R} , as stated below.

Theorem 2. *For any⁴ $\delta + \delta_s > 1$, $\lambda \geq 0$, the function $(\xi, \xi_{\perp}, \omega) \mapsto \mathcal{R}(\xi, \xi_{\perp}, \omega)$ has a unique minimizer in $\mathbb{R} \times \mathbb{R}_{\geq 0}^2$, which we denote by $(\xi^*, \xi_{\perp}^*, \omega^*)$. Define*

$$\mathcal{R}^*(\alpha) := (\xi^* - r)^2 + (\xi_{\perp}^*)^2 + (\omega^*)^2. \quad (25)$$

Consider the ridge regression estimator $\hat{\boldsymbol{\theta}}_{n,m}(\alpha)$ of Eq. (19). Assume $\|\boldsymbol{\theta}_\|_2 = r$, $\|\boldsymbol{\theta}_{*,s}\|_2 = r_s$ and $\langle \boldsymbol{\theta}_*, \boldsymbol{\theta}_{*,s} \rangle = \|\boldsymbol{\theta}_*\|_2 \|\boldsymbol{\theta}_{*,s}\|_2 \cos(\gamma)$, in the proportional asymptotics, $n, m, d \rightarrow \infty$ with $n/d \rightarrow \delta$, $m/d \rightarrow \delta_s$. Then, for any $\varepsilon, \varepsilon_0 > 0$, there exist $c > 0$ such that, for all n*

$$\mathbb{P}\left(\sup_{\alpha \in [\varepsilon_0, 1-\varepsilon_0]} |R(\hat{\boldsymbol{\theta}}_{m,n}(\alpha)) - \mathcal{R}^*(\alpha)| \leq \varepsilon\right) \geq 1 - 2e^{-cn}.$$

Further, we can take $\varepsilon_0 = 0$ if $\delta, \delta_s > 1$.

Remark 5.1 (Optimizing α over the validation set). Note that the concentration of $R(\hat{\boldsymbol{\theta}}_{m,n}(\alpha))$ around the theoretical prediction $\mathcal{R}^*(\alpha)$ in Theorem 2 is uniform over $\alpha \in [\varepsilon_0, 1 - \varepsilon_0]$. This means that we can find the optimal α by computing $\hat{\boldsymbol{\theta}}_{m,n}(\alpha)$ over a grid of α values, estimating $R(\hat{\boldsymbol{\theta}}_{m,n}(\alpha))$ over the validation set and choosing the optimal α . The uniform guarantee insures that this procedure will achieve risk $\min_{\alpha \in [0,1]} \mathcal{R}^*(\alpha) + o_P(1)$.

⁴We note in passing that the same proof, with some additional technical work, yields a characterization for $\delta + \delta_s \leq 1$ as well. We do not state it here because of space limits.

Remark 5.2 (Relation to scaling laws). An analysis of the equations for $(\xi^*, \xi_\perp^*, \omega^*)$ reveals that, for large δ, δ_s , the predicted excess risk behaves as $\mathcal{R}^*(\alpha) = \alpha^2 \mathcal{R}_{s,\infty}^* + \alpha^2 C_1 / \delta_s + (1 - \alpha)^2 C_2 / \delta_s + o(1/\delta, 1/\delta_s)$ (for some constants $\mathcal{R}_{s,\infty}^*, C_1, C_2$). This matches the low-dimensional asymptotics and our scaling law (5) with $\beta = 1$. In practice, we find that, for moderate δ, δ_s , the behavior of $\mathcal{R}^*(\alpha)$ is better approximated by a different value of β (see Appendix A.) Hence, we still use empirical values of β in applying the scaling law.

The last point is a general caveat about empirical scaling laws. Rather than exact asymptotics, these should be regarded as useful approximations in certain regimes.

6 Discussion

We conclude by discussing possible generalizations of the scaling law (5), and its applicability.

First, throughout this paper we assumed that $R_{\text{or}}^{\text{ex}}(\infty) = 0$, namely that we can achieve the Bayes error by training on infinitely many original samples. In practice this will not hold because of the limited model complexity. In standard scaling laws [KMH⁺20, HBM⁺22], this effect is accounted for by an additional term of the type $C \cdot N^{-\omega}$, in the excess test error, where N is the model size (number of parameters). In all of our experiments, we fixed N and focused on the dependence on the two sample sizes m, n and therefore ignored such a term, which is anyway negligible for the regimes we investigated empirically.

Second, the scaling law (5) implies as special cases that $R_{\text{or}}^{\text{ex}}(n) \approx A_{\text{or}} n^{-\beta}$, $R_{\text{su}}^{\text{ex}}(m) \approx R_{\text{su}}^{\text{ex}}(\infty) + A_{\text{su}} m^{-\beta}$. In particular, the exponent β is the same when training on real or surrogate data. In practice, we observe often two somewhat different exponents $\beta_{\text{or}} \neq \beta_{\text{su}}$. In these cases, we set $\beta = \beta_{\text{or}}$, and this appears to work reasonably well. However, we can imagine cases in which the difference between β_{or} and β_{su} is significant enough (5) will stop being accurate. It is not hard to propose generalizations of this law that can cover such cases: we defer this to future work.

Third, the applicability of Eq. (5), illustrated in Figs. 2 to 5 appears to be broader than what would be naively expected. Consider for instance Figure 5. In this case, the scaling of the original error $R_{\text{or}}^{\text{ex}}(n) \approx A_{\text{or}} n^{-\beta}$ only holds for $n/d \gg 1$ and requires $\beta = 1$. In contrast, we are applying Eq. (5) to $n/d = 2$ and with empirically determined $\beta \neq 1$. A possible explanation is that the two effect compensate: the empirically determined β captures the behavior in the regime of interest.

Of course, in order to be able to use the scaling law to predict how large the number of surrogate examples m should be, we need the empirical scaling of $R_{\text{su}}^{\text{ex}}(m)$ to be accurate.

Acknowledgements

We are grateful to Joseph Gardi, Germain Kolossov, Marc Laugharn, Kaleigh Mentzer, Rahul Ponnala, and Pulkit Tandon, for several conversations about this work. This work was carried out while Andrea Montanari was on leave from Stanford and a Chief Scientist at Granica (formerly known as Project N). The present research is unrelated to AM’s Stanford research.

References

- [AAMM⁺18] Hassan Abu Alhaja, Siva Karthik Mustikovela, Lars Mescheder, Andreas Geiger, and Carsten Rother, *Augmented reality meets computer vision: Efficient data generation for urban driving scenes*, International Journal of Computer Vision **126** (2018), 961–972.

- [ANZ22] Ibrahim M Alabdulmohsin, Behnam Neyshabur, and Xiaohua Zhai, *Revisiting neural scaling laws in language and vision*, Advances in Neural Information Processing Systems **35** (2022), 22300–22312.
- [Bir06] Steven Bird, *Nltk: the natural language toolkit*, Proceedings of the COLING/ACL 2006 Interactive Presentation Sessions, 2006, pp. 69–72.
- [BL96] Lawrence D Brown and Mark G Low, *Asymptotic equivalence of nonparametric regression and white noise*, The Annals of Statistics **24** (1996), no. 6, 2384–2398.
- [CLCG19] Yuhua Chen, Wen Li, Xiaoran Chen, and Luc Van Gool, *Learning semantic segmentation from synthetic data: A geometrically guided input-output adaptation approach*, Proceedings of the IEEE/CVF conference on computer vision and pattern recognition, 2019, pp. 1841–1850.
- [FCK⁺23] Lijie Fan, Kaifeng Chen, Dilip Krishnan, Dina Katabi, Phillip Isola, and Yonglong Tian, *Scaling laws of synthetic images for model training... for now*, arXiv preprint arXiv:2312.04567 (2023).
- [Gor85] Yehoram Gordon, *Some inequalities for gaussian processes and applications*, Israel Journal of Mathematics **50** (1985), no. 4, 265–289.
- [HBM⁺22] Jordan Hoffmann, Sebastian Borgeaud, Arthur Mensch, Elena Buchatskaya, Trevor Cai, Eliza Rutherford, Diego de Las Casas, Lisa Anne Hendricks, Johannes Welbl, Aidan Clark, et al., *Training compute-optimal large language models*, arXiv preprint arXiv:2203.15556 (2022).
- [HKHM21] Danny Hernandez, Jared Kaplan, Tom Henighan, and Sam McCandlish, *Scaling laws for transfer*, arXiv preprint arXiv:2102.01293 (2021).
- [HKK⁺20] Tom Henighan, Jared Kaplan, Mor Katz, Mark Chen, Christopher Hesse, Jacob Jackson, Heewoo Jun, Tom B Brown, Prafulla Dhariwal, Scott Gray, et al., *Scaling laws for autoregressive generative modeling*, arXiv preprint arXiv:2010.14701 (2020).
- [HNA⁺17] Joel Hestness, Sharan Narang, Newsha Ardalani, Gregory Diamos, Heewoo Jun, Hassan Kianinejad, Md Mostofa Ali Patwary, Yang Yang, and Yanqi Zhou, *Deep learning scaling is predictable, empirically*, arXiv preprint arXiv:1712.00409 (2017).
- [HNK⁺22] Xuanli He, Islam Nassar, Jamie Kiros, Gholamreza Haffari, and Mohammad Norouzi, *Generate, annotate, and learn: Nlp with synthetic text*, Transactions of the Association for Computational Linguistics **10** (2022), 826–842.
- [HSY⁺22] Ruifei He, Shuyang Sun, Xin Yu, Chuhui Xue, Wenqing Zhang, Philip Torr, Song Bai, and Xiaojuan Qi, *Is synthetic data from generative models ready for image recognition?*, arXiv preprint arXiv:2210.07574 (2022).
- [JRBM⁺17] Matthew Johnson-Roberson, Charles Barto, Rounak Mehta, Sharath Nittur Sridhar, Karl Rosaen, and Ram Vasudevan, *Driving in the matrix: Can virtual worlds replace human-generated annotations for real world tasks?*, 2017 IEEE International Conference on Robotics and Automation (ICRA), IEEE, 2017, pp. 746–753.

- [KMH⁺20] Jared Kaplan, Sam McCandlish, Tom Henighan, Tom B Brown, Benjamin Chess, Rewon Child, Scott Gray, Alec Radford, Jeffrey Wu, and Dario Amodei, *Scaling laws for neural language models*, arXiv preprint arXiv:2001.08361 (2020).
- [MHZH22] Yu Meng, Jiaxin Huang, Yu Zhang, and Jiawei Han, *Generating training data with language models: Towards zero-shot language understanding*, Advances in Neural Information Processing Systems **35** (2022), 462–477.
- [MM21] Léo Miolane and Andrea Montanari, *The distribution of the lasso: Uniform control over sparse balls and adaptive parameter tuning*, The Annals of Statistics **49** (2021), no. 4, 2313–2335.
- [MPRP16] Andreas Maurer, Massimiliano Pontil, and Bernardino Romera-Paredes, *The benefit of multitask representation learning*, Journal of Machine Learning Research **17** (2016), no. 81, 1–32.
- [MPT⁺22] Arthur Moreau, Nathan Piasco, Dzmitry Tsishkou, Bogdan Stanciulescu, and Arnaud de La Fortelle, *Lens: Localization enhanced by nerf synthesis*, Conference on Robot Learning, PMLR, 2022, pp. 1347–1356.
- [MRB⁺23] Niklas Muennighoff, Alexander M Rush, Boaz Barak, Teven Le Scao, Aleksandra Piktus, Nouamane Tazi, Sampo Pyysalo, Thomas Wolf, and Colin Raffel, *Scaling data-constrained language models*, arXiv preprint arXiv:2305.16264 (2023).
- [Rei08] Markus Reiß, *Asymptotic equivalence for nonparametric regression with multivariate and random design*, The Annals of Statistics (2008), 1957–1982.
- [RRBS19] Jonathan S Rosenfeld, Amir Rosenfeld, Yonatan Belinkov, and Nir Shavit, *A constructive prediction of the generalization error across scales*, International Conference on Learning Representations, 2019.
- [RSM⁺16] German Ros, Laura Sellart, Joanna Materzynska, David Vazquez, and Antonio M Lopez, *The synthia dataset: A large collection of synthetic images for semantic segmentation of urban scenes*, Proceedings of the IEEE conference on computer vision and pattern recognition, 2016, pp. 3234–3243.
- [SLW20] Viktor Seib, Benjamin Lange, and Stefan Wirtz, *Mixing real and synthetic data to enhance neural network training—a review of current approaches*, arXiv preprint arXiv:2007.08781 (2020).
- [TAH18] Christos Thrampoulidis, Ehsan Abbasi, and Babak Hassibi, *Precise error analysis of regularized m -estimators in high dimensions*, IEEE Transactions on Information Theory **64** (2018), no. 8, 5592–5628.
- [TDR⁺21] Yi Tay, Mostafa Dehghani, Jinfeng Rao, William Fedus, Samira Abnar, Hyung Won Chung, Sharan Narang, Dani Yogatama, Ashish Vaswani, and Donald Metzler, *Scale efficiently: Insights from pretraining and finetuning transformers*, International Conference on Learning Representations, 2021.
- [TJJ20] Nilesh Tripuraneni, Michael Jordan, and Chi Jin, *On the theory of transfer learning: The importance of task diversity*, Advances in neural information processing systems **33** (2020), 7852–7862.

- [TOH15] Christos Thrampoulidis, Samet Oymak, and Babak Hassibi, *Regularized linear regression: A precise analysis of the estimation error*, Proceedings of Machine Learning Research **40** (2015), 1683–1709.
- [TPA⁺18] Jonathan Tremblay, Aayush Prakash, David Acuna, Mark Brophy, Varun Jampani, Cem Anil, Thang To, Eric Cameracci, Shaad Boochoon, and Stan Birchfield, *Training deep networks with synthetic data: Bridging the reality gap by domain randomization*, Proceedings of the IEEE conference on computer vision and pattern recognition workshops, 2018, pp. 969–977.
- [Tsy09] Alexandre B. Tsybakov, *Introduction to nonparametric estimation*, Springer, 2009.
- [vdV00] Aad W van der Vaart, *Asymptotic statistics*, Cambridge University Press, 2000.
- [Ver18] Roman Vershynin, *High-dimensional probability: An introduction with applications in data science*, vol. 47, Cambridge university press, 2018.
- [YCFB⁺22] Lin Yen-Chen, Pete Florence, Jonathan T Barron, Tsung-Yi Lin, Alberto Rodriguez, and Phillip Isola, *Nerf-supervision: Learning dense object descriptors from neural radiance fields*, 2022 International Conference on Robotics and Automation (ICRA), IEEE, 2022, pp. 6496–6503.

A Details of empirical results

A.1 Binary classification with Gaussian mixture data

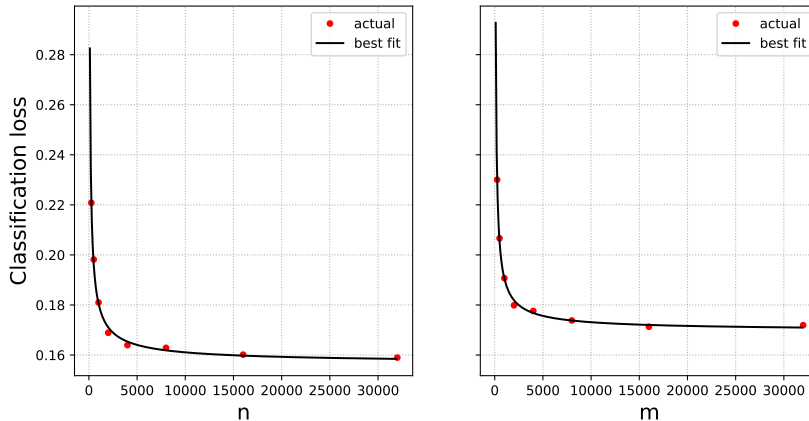


Figure 6: Gaussian mixture data and logistic regression. Test error when trained on original (left plot) and surrogate (right plot) data only (red dots). Best fits of the form are shown in blue. These gives the estimates $\beta = 0.72$, $R_* = 0.157$, and $R_{\text{su}}^{\text{ex}}(\infty) = 0.013$.

We provide details for the models used in the simulations of Section A.1.

Logistic regression: We use the scikit-learn implementation with the lbfgs solver, fitting the intercept, with maximum iterations set to 10k. For each run of each (m, n, α) combination, we set the ℓ_2 penalty (parameter C in scikit-learn) to $2^i, i = -8, \dots, 8$ and $10^i, i = -6, -5, -4, -3, 3, 4, 5, 6$, and only report the test result for the value that achieves the best validation error. The results results of the individual scaling law estimates and the comparison of joint training results with the scaling law predictions are shown in Figures 6 and 7.

Neural network: The network has one hidden layer with 32 ReLU neurons, and an output neuron using sigmoid. For training we use the binary cross entropy loss, a constant learning rate of 0.05, and batch size 64. We train the network for 1,000 epochs. Similar to the procedure in logistic regression, we use ℓ_2 regularization (weight decay) and use the validation set to choose the best regularization parameter from the set $\{0, 10^{-5}, 10^{-4}, 10^{-3}, 2 \cdot 10^{-3}, 4 \cdot 10^{-3}, 10^{-2}, 2 \cdot 10^{-2}, 4 \cdot 10^{-2}, 10^{-1}, 2 \cdot 10^{-1}, 4 \cdot 10^{-1}\}$.

A.2 Sentiment analysis in movie reviews

To convert the movie reviews to vectors, we use a combination of two different embedding: We use all the reviews in the training data and then use nltk tagger [Bir06] to find the most frequent 500 adjectives appearing in the samples used for training. Then we use the common Tfidf vectorizer (we used scikit-learn’s implementation of tfidf vectorizer) for which we use the list of these most common 500 adjectives as vocabulary. This gives us a vector of length 500 dimension for each review. In addition, we also apply “Paraphrase-MiniLM-L6-v2” sentence transformer which is based on BERT with 6 Transformer Encoder Layers, and return a 384 dimension vector representation of the reviews. For each movie review we concatenate the results of tfidf vectorizer and sentence transformer to get a 884 dimensional representation that we use as our input vector.

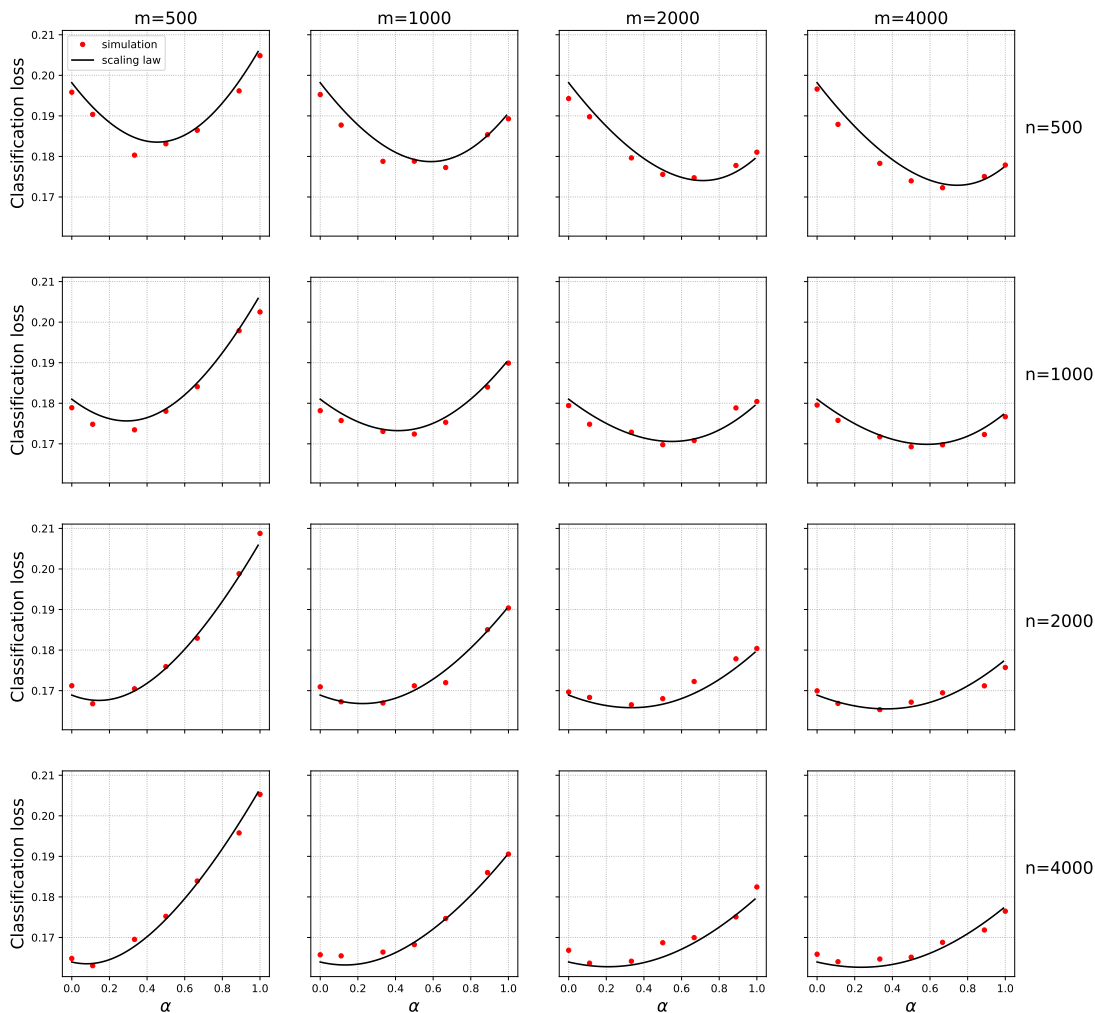


Figure 7: Gaussian mixture data and logistic regression. Test error when trained on mixtures of original (n varying by row) and surrogate (m varying by column) data. Black curves: scaling formula (5).

We use logistic regression and neural networks with the same set of parameters as in the Gaussian mixture experiments (except for the input dimension).

Results omitted from the main text are presented in Figures 8–10.

A.3 Image classification with CIFAR10 and CIFAR100

We largely use the model and the training procedure described at <https://jovian.ml/aakashns/05b-cifar10-resnet>. We normalize the images for mean and standard deviation. We train a 9-layer ResNet model for classification, using Adam for optimization, weight decay, and gradient clipping, trained over 16 epochs with a one-cycle learning rate scheduling policy, minimizing cross entropy loss. For each combination of m , n , and α , we report the average test error over 10 runs. Since there is no overlap between the label sets of CIFAR10 and CIFAR100, the latter dataset needs to be relabeled. We do this by training a separate 9-layer ResNet model on 10,000 randomly chosen CIFAR10 images from the training set of 50,000 examples (without creating a separate split for

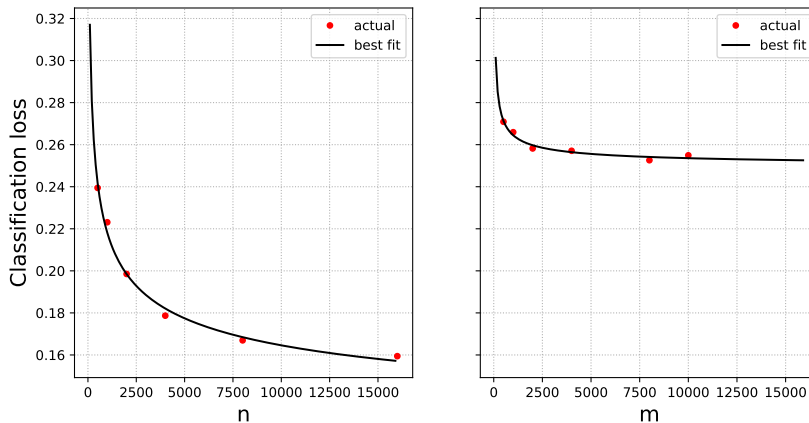


Figure 8: IMDB and Rotten Tomatoes data and logistic regression. Test error when trained on original (left plot) and surrogate (right plot) data only (red dots), together with scaling law fits. Best fit parameters are $\beta = 0.27$, $R_* = 0.101$ and $R_{\text{su}}^{\text{ex}}(\infty) = 0.148$.

them), and use its predictions on CIFAR100 images as labels.

Scaling curves are presented in Figure 11.

A.4 High-dimensional ridge regression

We present additional ridge regression experiments here in Figs. 12–23. In these experiments, as in the main paper, we set $d = 500$, $\sigma^2 = \sigma_s^2 = 1$, $\|\boldsymbol{\theta}_*\| = 1$, $\|\boldsymbol{\theta}_{*,s}\| = 1$, except for the last four Figs. 20–23, where we use $\|\boldsymbol{\theta}_{*,s}\| = 1/2$. We used angle $\gamma = \pi/6$ and $\pi/2$ in our experiments.

We consider two methods: (1) Fix λ to a very small value 2^{-10} , and (2) For each random draw of datasets select λ that achieves the best validation performance. For the latter method, we tried $\lambda = 2^i$, where $i = -10, -8, -6, \dots, 8, 10$. For ridge regression simulations, we directly plot the excess test risks, as the parameter $\boldsymbol{\theta}$ for original data is known and for any $\hat{\boldsymbol{\theta}}$ the excess test risk in this model is $\|\boldsymbol{\theta} - \hat{\boldsymbol{\theta}}\|^2$.

B Low-dimensional asymptotics: Proofs for Section 3

Before proving Proposition 3.1, we state the regularity assumptions. (Here and in the following $\mathbf{B}(\boldsymbol{\theta}_*, r)$ is the ball of radius r centered at $\boldsymbol{\theta}_*$.)

Assumption 2 (‘Classical’ regularity). *We assume the following:*

- (a) *The original population risk $R(\boldsymbol{\theta})$ is uniquely minimized at a point $\boldsymbol{\theta}_*$.*
- (b) *$\boldsymbol{\theta} \mapsto \ell(\boldsymbol{\theta}; \mathbf{z})$ is non-negative lower semicontinuous. Further, define the following limit in $[0, \infty]$ for $\mathbf{u} \in \mathbb{S}^{d-1}$:*

$$\ell_\infty(\mathbf{u}; \mathbf{z}) := \liminf_{\substack{\boldsymbol{\theta} \rightarrow \infty \\ \boldsymbol{\theta}/\|\boldsymbol{\theta}\|_2 \rightarrow \mathbf{u}}} \ell(\boldsymbol{\theta}; \mathbf{z}). \quad (26)$$

Then we assume $\inf_{\mathbf{u} \in \mathbb{S}^{d-1}} \mathbb{E} \ell_\infty(\mathbf{u}; \mathbf{z}) \geq R(\boldsymbol{\theta}_) + c$ for some $c > 0$.*

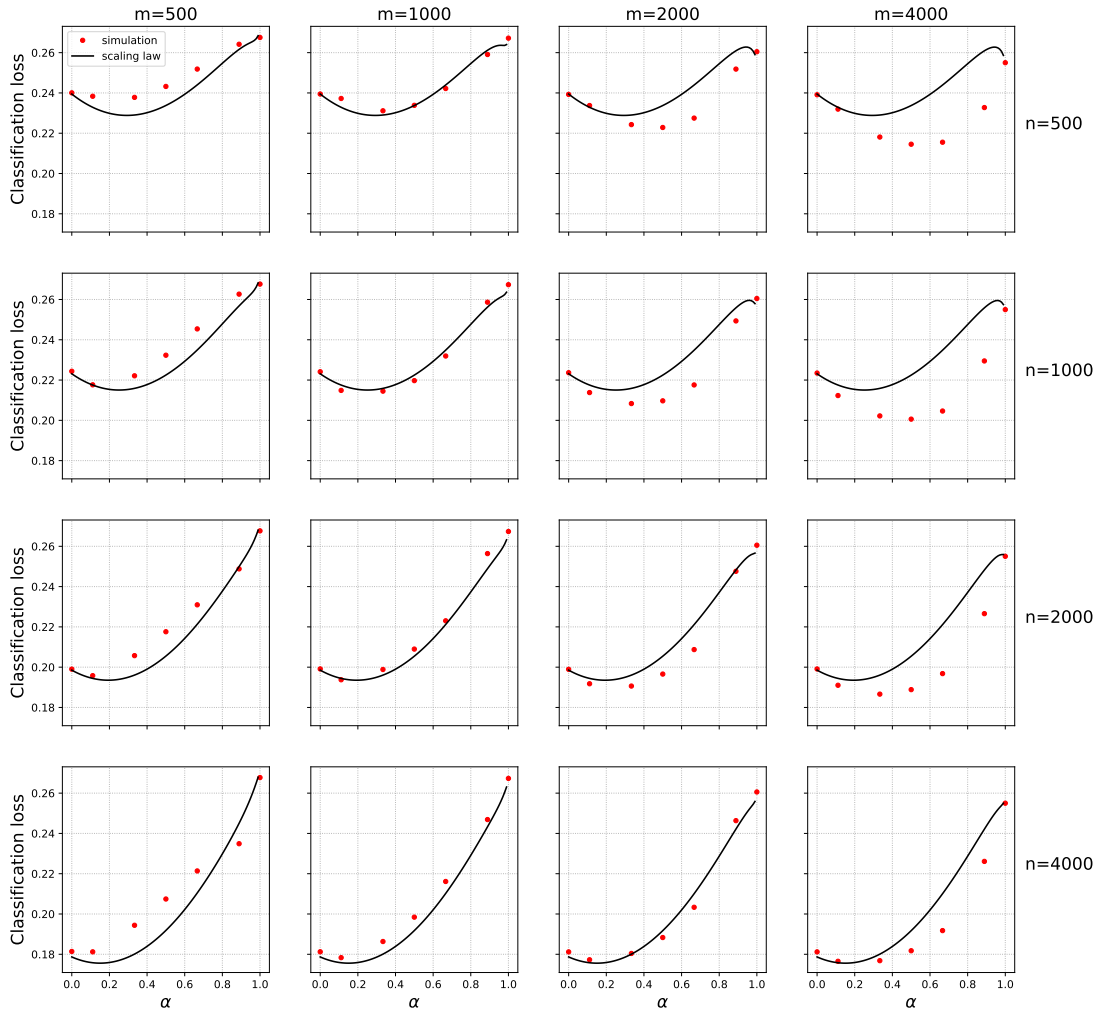


Figure 9: IMDB and Rotten Tomatoes data and logistic regression. Test error when trained on mixtures of original and surrogate data. Black curves: prediction from Eq. (5).

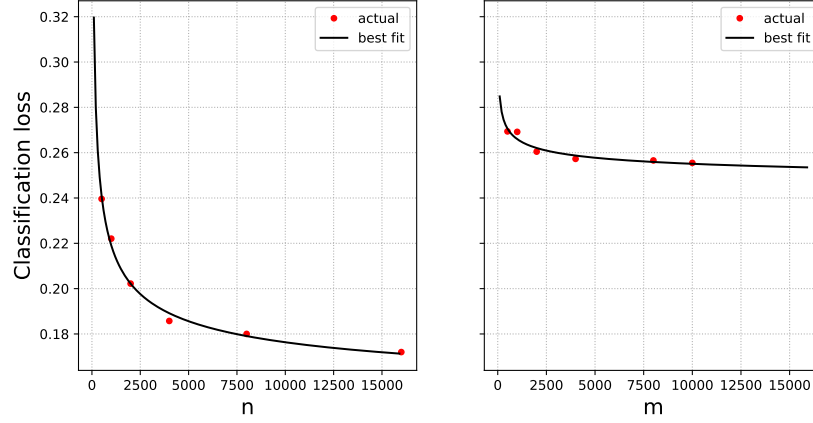


Figure 10: IMDB and Rotten Tomatoes data and neural networks. Scaling law fits for models trained on original (left plot) and surrogate (right plot) data only (red dots)(as in Fig. 8.) Best fit parameters are $\beta = 0.37$, $R_* = 0.145$ and $R_{su}^{ex}(\infty) = 0.095$.

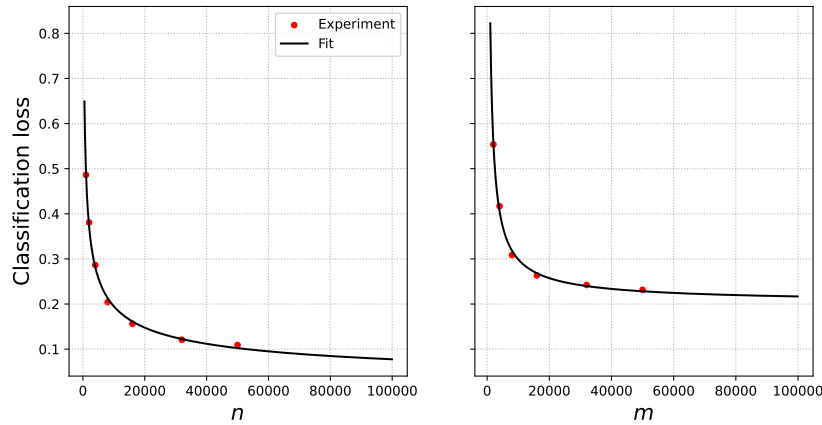


Figure 11: CIFAR10 and CIFAR100 data: (left) Test error scaling of original data (left) and surrogate data (right). Best fit parameters are $\beta = 0.404$, $R_* = 0.0013$, and $R_{su}^{ex}(\infty) = 0.199$.

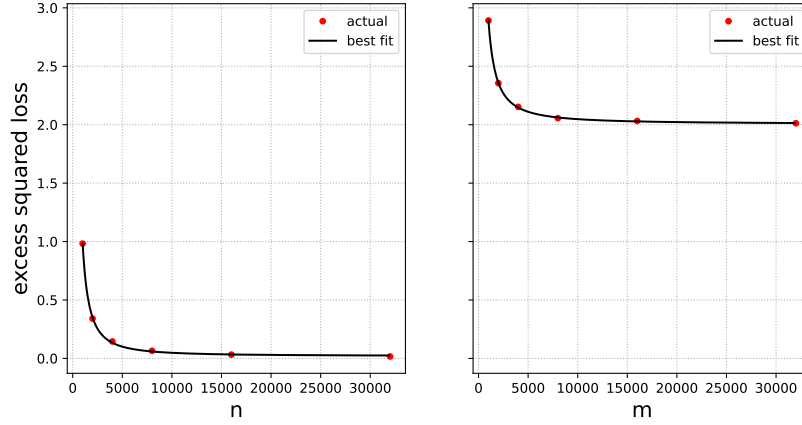


Figure 12: Ridge regression with $\gamma = \pi/2$, and regularization parameter $\lambda = 2^{-10}$: Test error scaling of the original data (left), and surrogate data (right). Best curve fits give the estimates $\beta = 1.57$ and $R_{su}^{\text{ex}}(\infty) = 2.0$

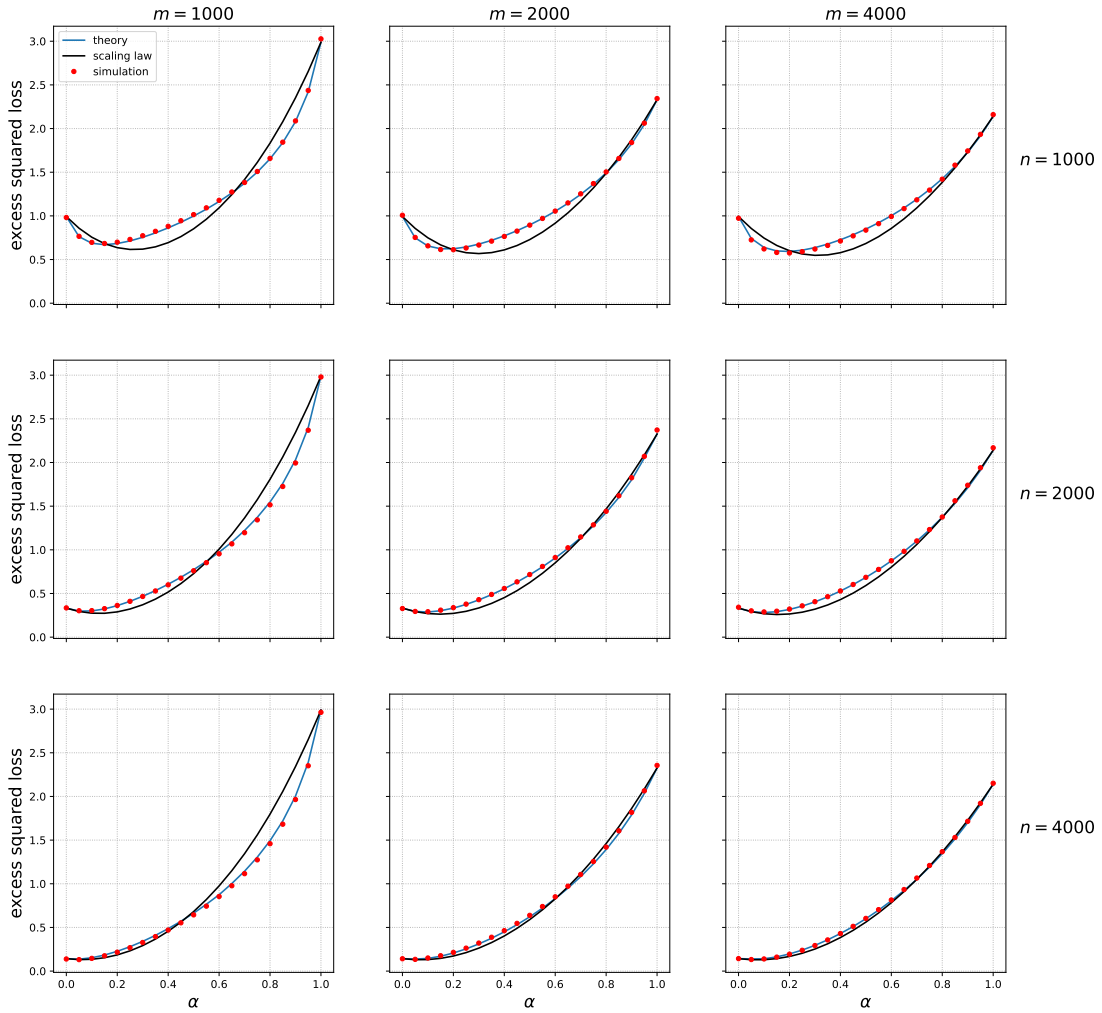


Figure 13: Ridge regression with $\gamma = \pi/2$, and regularization parameter $\lambda = 2^{-10}$

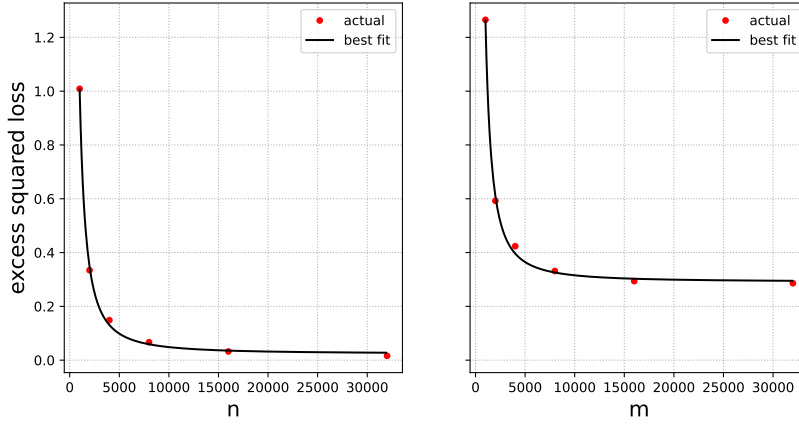


Figure 14: Ridge regression with $\pi/6$ between θ and θ_s , and regularization parameter $\lambda = 2^{-10}$: Test error scaling of the original data (left), and surrogate data (right). Best curve fits give the estimates $\beta = 1.57$ and $R_{\text{su}}^{\text{ex}}(\infty) = 0.29$

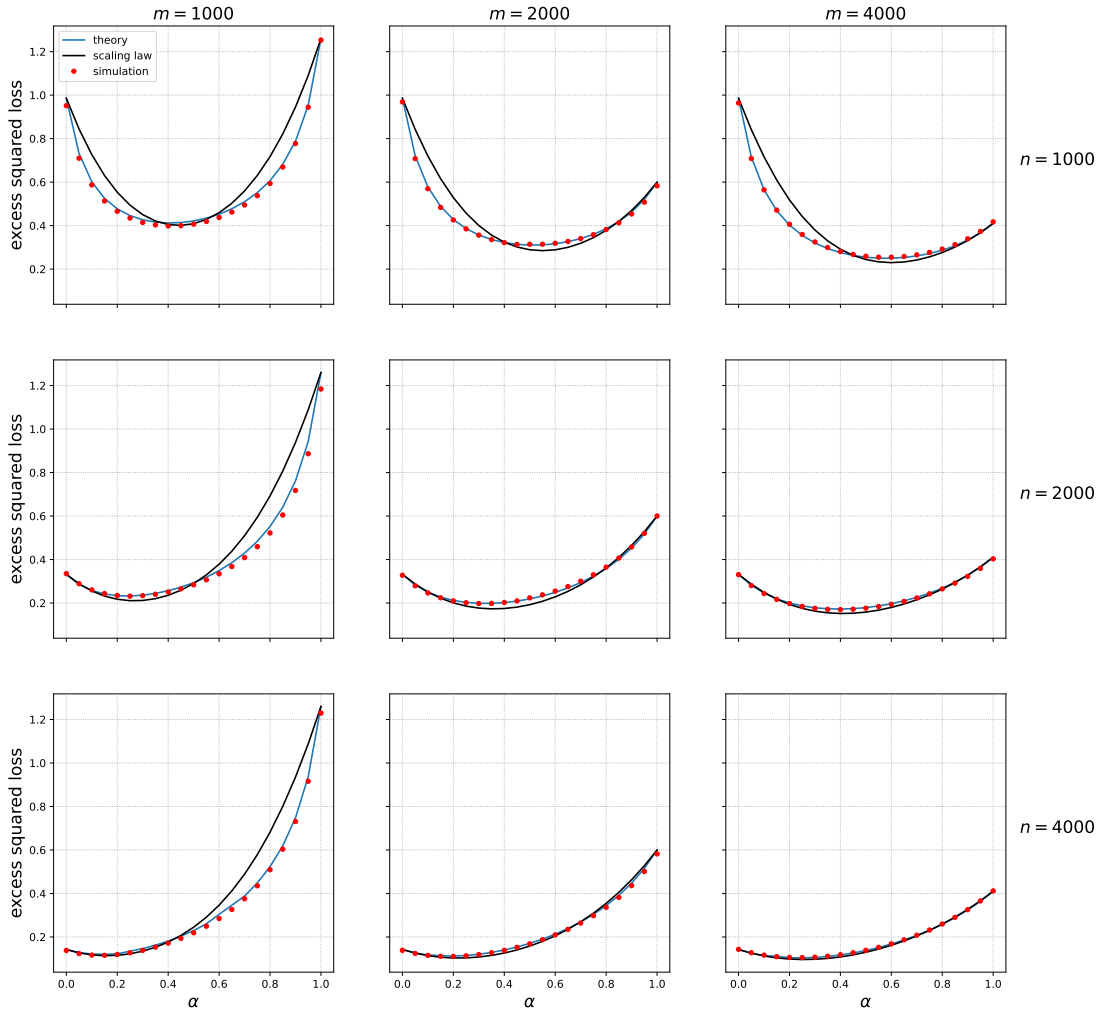


Figure 15: Ridge regression with $\pi/6$ between θ and θ_s , and regularization parameter $\lambda = 2^{-10}$

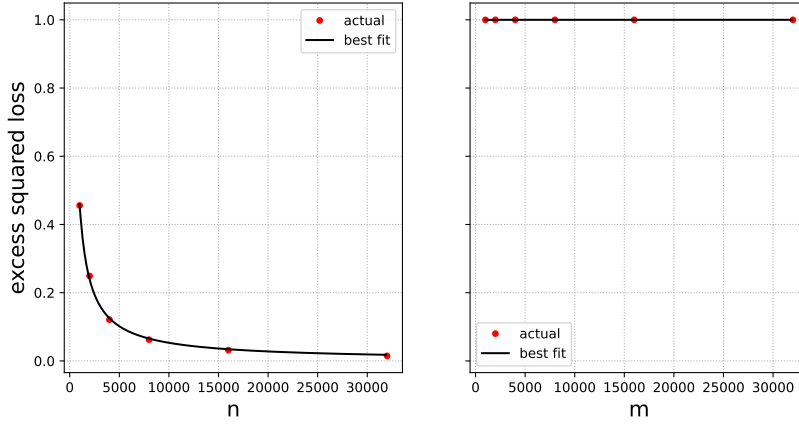


Figure 16: Ridge regression with $\pi/2$ between θ and θ_s , and the best regularization parameter: Test error scaling of the original data (left), and surrogate data (right). Best curve fits give the estimates $\beta = 0.94$ and $R_{\text{su}}^{\text{ex}}(\infty) = 1.0$

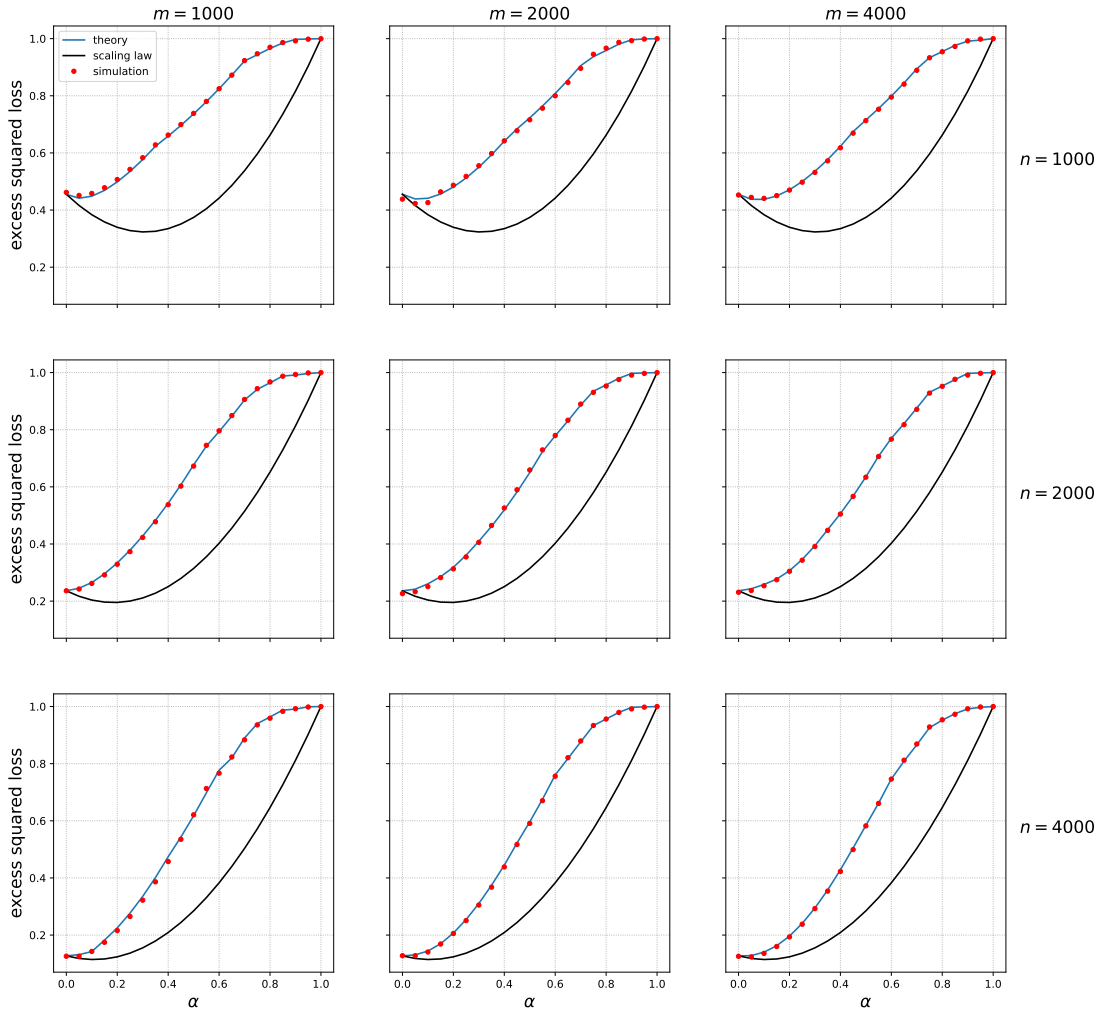


Figure 17: Ridge regression with $\gamma = \pi/2$, and the best regularization parameter

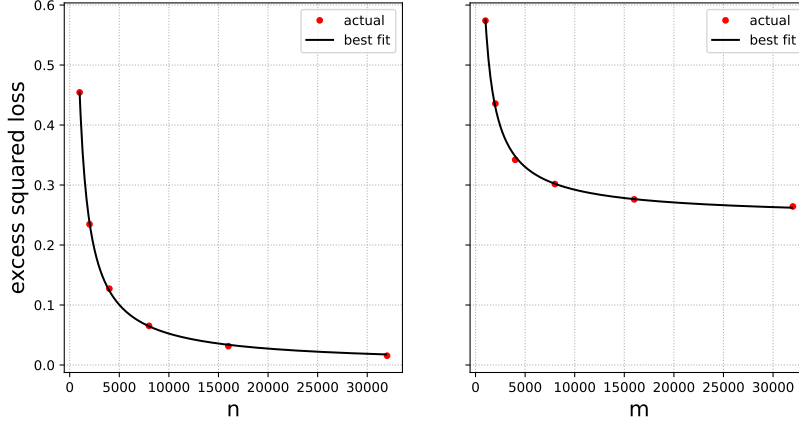


Figure 18: Ridge regression with $\pi/6$ between θ and θ_s , and the best regularization parameter: Test error scaling of the original data (left), and surrogate data (right). Best curve fits give the estimates $\beta = 0.94$ and $R_{\text{su}}^{\text{ex}}(\infty) = 0.24$

- (c) $\theta \mapsto \ell(\theta; \mathbf{z})$ is differentiable at θ_* almost surely, both under $\mathbf{z} \sim \mathbb{P}$ and under $\mathbf{z} \sim \mathbb{P}^s$. Further, there exists $r > 0$ such that, letting $\mathbf{B} := \mathbf{B}(\theta_*, r)$, the following holds for a constant C :

$$\mathbb{E} \sup_{\theta_1 \neq \theta_2 \in \mathbf{B}} \left\{ \frac{|\ell(\theta_1; \mathbf{z}) - \ell(\theta_2; \mathbf{z})|^2}{\|\theta_1 - \theta_2\|_2^2} \right\} \leq C < \infty. \quad (27)$$

- (d) The functions $\theta \mapsto R(\theta)$, $\theta \mapsto R^s(\theta)$, are twice differentiable in a neighborhood of θ_* , with Lipschitz continuous Hessian. Further $\nabla^2 R(\theta_*) \succ \mathbf{0}$ (strictly positive definite).

Lemma B.1. Under the assumptions of Proposition 3.1 (Assumption 1 and Assumption 2) there exists $\alpha_{\max} \in (0, 1]$, depending only on the constants appearing there such that the following holds:

- (i) The function $\theta \mapsto R(\theta; \alpha) := (1 - \alpha)R(\theta) + \alpha R^s(\theta)$ has a unique minimizer $\theta_*(\alpha) \in \mathbb{R}^d$. Further $\theta_*(\alpha) \in \mathbf{B}(\theta_*, r)$, and $\theta_*(\alpha) \rightarrow \theta_*$ as $\alpha \downarrow 0$.
- (ii) We have $\hat{\theta}_{m,n}(\alpha) \rightarrow \theta_*$ in probability as $m, n \rightarrow \infty$.

Proof. Fix $r_0 \in (0, r]$ By Assumption 2.(a), $\inf_{\theta \notin \mathbf{B}(\theta_*, r_0)} R(\theta) > R(\theta_*) + \delta_0$ for some constant δ_0 . Hence, using Assumption 1, for any $\theta \notin \mathbf{B}(\theta_*, r)$

$$\begin{aligned} R(\theta; \alpha) &\geq R(\theta) - K_*\alpha[1 + R(\theta)] \\ &\geq (1 - K_*\alpha)R(\theta) - K_*\alpha \\ &\geq (1 - K_*\alpha)(R(\theta_*) + \delta_0) - K_*\alpha. \end{aligned}$$

In the other hand $R(\theta_*; \alpha) \leq (1 + K_*\alpha)R(\theta_*) + K_*\alpha$, whence

$$\begin{aligned} R(\theta; \alpha) - R(\theta_*; \alpha) &\geq (1 - K_*\alpha)\delta_0 - 2K_*\alpha R(\theta_*) \\ &\quad - 2K_*\alpha, \end{aligned}$$

which is strictly positive for $\alpha < \alpha_{\max}(r_0) := \delta_0 / (4K_*(1 + R(\theta_*)))$. Hence the minimum must be achieved in $\mathbf{B}(\theta_*; r_0)$ (note that since $R(\theta)$, $R_s(\theta)$ are lower semicontinuous, the minimum is achieved).

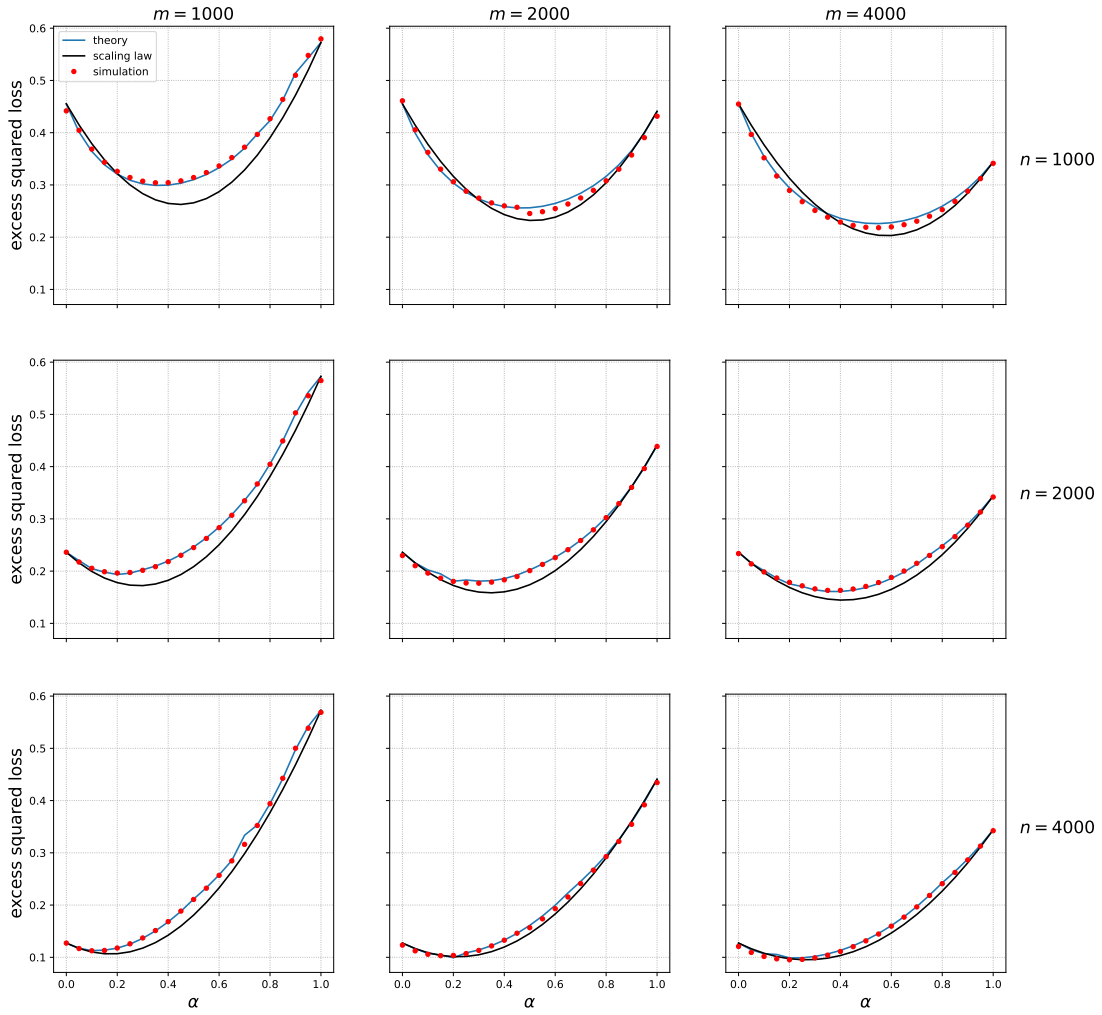


Figure 19: Ridge regression with $\pi/6$ between θ and θ_s , and the best regularization parameter

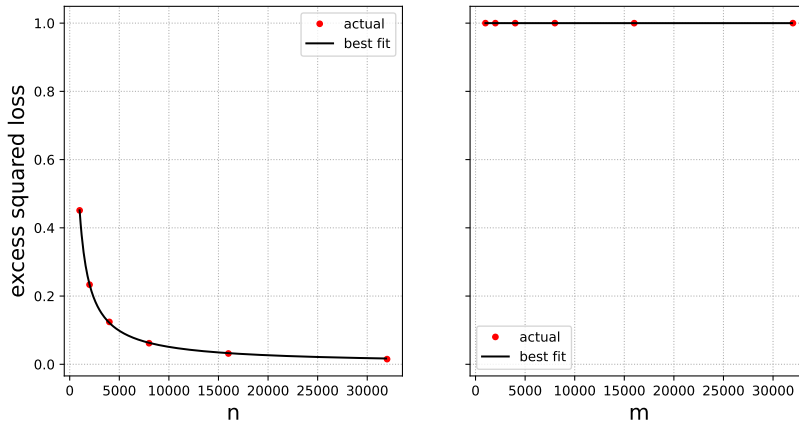


Figure 20: Ridge regression with $\pi/2$ between θ and θ_s , $\|\theta\| = 1$, $\|\theta_s\| = 1/2$ and the best regularization parameter: Test error scaling of the original data (left), and surrogate data (right). Best curve fits give the estimates $\beta = 0.94$ and $R_{su}^{ex}(\infty) = 1.00$

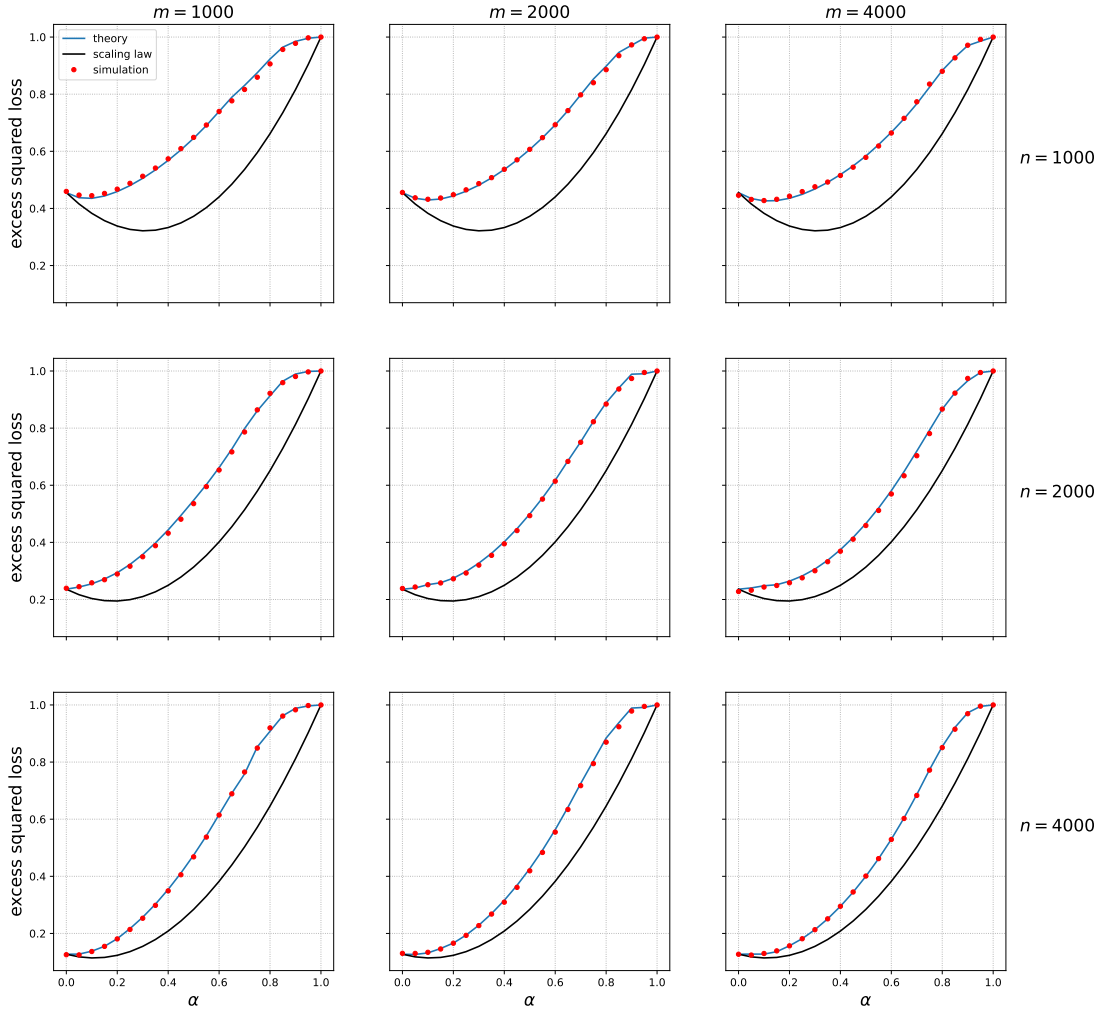


Figure 21: Ridge regression with $\pi/2$ between θ and θ_s , $\|\theta\| = 1$, $\|\theta_s\| = 1/2$ and the best regularization parameter

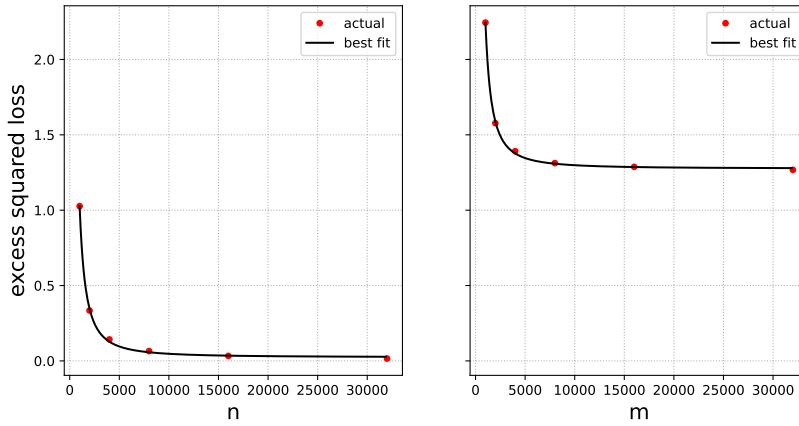


Figure 22: Ridge regression with $\gamma = \pi/2$, $\|\theta\| = 1$, $\|\theta_s\| = 1/2$, and regularization parameter $\lambda = 2^{-10}$: Test error scaling of the original data (left), and surrogate data (right). Best curve fits give the estimates $\beta = 1.57$ and $R_{\text{su}}^{\text{ex}}(\infty) = 1.27$

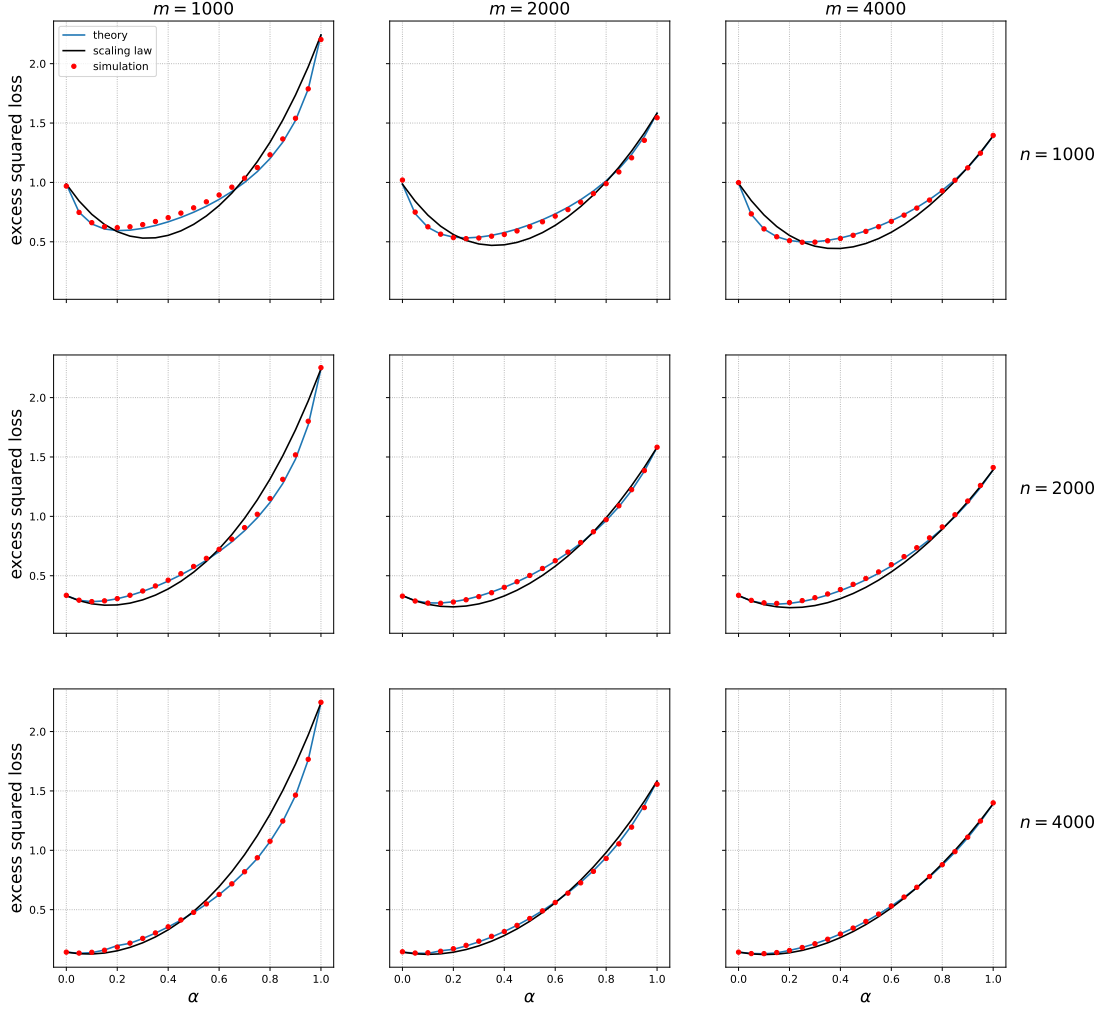


Figure 23: Ridge regression with $\gamma = \pi/2$, $\|\theta\| = 1$, $\|\theta_s\| = 1/2$, and regularization parameter $\lambda = 2^{-10}$

By Assumption 2.(d), for r_0 sufficiently small, $\theta \mapsto \nabla R(\theta; \alpha)$ is strictly convex in $\mathbf{B}(\theta_*; r_0)$ and therefore the minimizer is unique. This proves point (i).

Point (ii) follows from a modification of Theorem 5.14 in [vdV00]. Namely, for a diverging sequence $\{(m(k), n(k)) : k \in \mathbb{N}\}$, we consider to $\hat{R}_{*,k}(\mathbf{u}) := \hat{R}_{m(k),n(k)}(c(\mathbf{u})\mathbf{u}; \alpha)$, where $c(\mathbf{u}) := (1 + \|\mathbf{u}\|^2)^{-1/2}$. This function is lower semicontinuous on the compact set $\mathbf{B}(\mathbf{0}; 1)$ and converges almost surely to its expectation for every fixed \mathbf{u} in this set, and hence the argument of Theorem 5.14 [vdV00] applies here. \square

Proof of Proposition 3.1. By a modification of Theorem 5.39 in [vdV00] (here $\theta_*(\alpha)$ is defined as in Lemma B.1)

$$\hat{\theta}_{m,n}(\alpha) = \theta_*(\alpha) + \frac{1-\alpha}{n} \mathbf{H}(\alpha)^{-1} \sum_{i=1}^n [\nabla \ell(\theta_*(\alpha); \mathbf{z}_i) - \mathbb{E} \nabla \ell(\theta; \mathbf{z})] \quad (28)$$

$$+ \frac{\alpha}{m} \mathbf{H}(\alpha)^{-1} \sum_{i=1}^m [\nabla \ell(\theta_*(\alpha); \mathbf{z}_i^c) - \mathbb{E}_s \nabla \ell(\theta; \mathbf{z})] + O_P(m^{-1} + n^{-1}), \quad (29)$$

where $\mathbf{H}(\alpha) := (1 - \alpha)\nabla^2 R(\boldsymbol{\theta}_*(\alpha)) + \alpha\nabla^2 R_s(\boldsymbol{\theta}_*(\alpha))$. Note that in the present setting the error is of order $m^{-1} + n^{-1}$ because we assume the Hessian to be Lipschitz continuous.

The population minimizer $\boldsymbol{\theta}_*(\alpha)$ solves

$$\begin{aligned} \mathbf{0} &= \nabla R(\boldsymbol{\theta}_*(\alpha); \alpha) \\ &= \nabla R(\boldsymbol{\theta}_*; \alpha) + \nabla^2 R(\boldsymbol{\theta}_*; \alpha)(\boldsymbol{\theta}_*(\alpha) - \boldsymbol{\theta}_*) + \int_0^1 [\nabla^2 R(\boldsymbol{\theta}_t; \alpha) - \nabla^2 R(\boldsymbol{\theta}_*; \alpha)](\boldsymbol{\theta}_*(\alpha) - \boldsymbol{\theta}_*) dt, \end{aligned}$$

where $\boldsymbol{\theta}_t = t\boldsymbol{\theta}_*(\alpha) + (1-t)\boldsymbol{\theta}_*$. Denoting by L_2 the Lipschitz constant of the Hessian (in operator norm), and recalling that $\nabla R(\boldsymbol{\theta}_*) = \mathbf{0}$, we have

$$\begin{aligned} \nabla^2 R(\boldsymbol{\theta}_*; \alpha)(\boldsymbol{\theta}_*(\alpha) - \boldsymbol{\theta}_*) &= -\alpha\nabla R_s(\boldsymbol{\theta}_*) + \mathbf{u}, \\ \|\mathbf{u}\|_2 &\leq L_2\|\boldsymbol{\theta}_*(\alpha) - \boldsymbol{\theta}_*\|^2. \end{aligned}$$

Recalling that, by Lemma B.1, $\boldsymbol{\theta}_*(\alpha) \rightarrow \boldsymbol{\theta}_*$ as $\alpha \rightarrow 0$, this implies

$$\boldsymbol{\theta}_*(\alpha) - \boldsymbol{\theta}_* = -\mathbf{H}^{-1}\nabla R_s(\boldsymbol{\theta}_*)\alpha + O(\left(\|\nabla R_s(\boldsymbol{\theta}_*)\|_2 \vee \|\nabla R_s(\boldsymbol{\theta}_*)\|_2^2\right)\alpha^2). \quad (30)$$

Substituting in Eq. (28), we get

$$\hat{\boldsymbol{\theta}}_{m,n}(\alpha) - \boldsymbol{\theta}_* = -\mathbf{H}^{-1}\nabla R_s(\boldsymbol{\theta}_*)\alpha + \frac{1-\alpha}{n}\mathbf{H}(\alpha)^{-1}\sum_{i=1}^n [\nabla\ell(\boldsymbol{\theta}_*(\alpha); \mathbf{z}_i) - \mathbb{E}\nabla\ell(\boldsymbol{\theta}; \mathbf{z})] \quad (31)$$

$$+ \frac{\alpha}{m}\mathbf{H}(\alpha)^{-1}\sum_{i=1}^m [\nabla\ell(\boldsymbol{\theta}_*(\alpha); \mathbf{z}_i^c) - \mathbb{E}_s\nabla\ell(\boldsymbol{\theta}; \mathbf{z})] + \boldsymbol{\Delta}, \quad (32)$$

$$\|\boldsymbol{\Delta}\| \leq C\left(\|\nabla R_s(\boldsymbol{\theta}_*)\|_2 \vee \|\nabla R_s(\boldsymbol{\theta}_*)\|_2^2\right)\alpha^2 + \frac{C}{m \wedge n}. \quad (33)$$

The claim follows by substituting the above in

$$\mathbb{E}R(\hat{\boldsymbol{\theta}}_{m,n}(\alpha)) - R(\boldsymbol{\theta}) = \mathbb{E}\langle \hat{\boldsymbol{\theta}}_{m,n}(\alpha) - \boldsymbol{\theta}_*, \mathbf{H}(\hat{\boldsymbol{\theta}}_{m,n}(\alpha) - \boldsymbol{\theta}_*) \rangle + O\left(\mathbb{E}\|\hat{\boldsymbol{\theta}}_{m,n}(\alpha) - \boldsymbol{\theta}_*\|^3\right) \quad (34)$$

and using $\mathbf{H}(\alpha) = \mathbf{H} + O(\alpha)$. \square

C Analysis of the nonparametric model: Proofs for Section 4

The proof of Theorem 1 is based on a reduction to a suitable ‘sequence model’ via the Fourier transform, defined as

$$\theta(\mathbf{q}) := \int_{[0,1]^d} f(\mathbf{x}) e^{-\iota\langle \mathbf{q}, \mathbf{x} \rangle} d\mathbf{x}, \quad (35)$$

for $\mathbf{q} \in \mathcal{Q}_d := \{2\pi\mathbf{q} : \mathbf{q} \in \mathbb{Z}^d\}$, where $\iota = \sqrt{-1}$. The inverse Fourier transform is defined as

$$f(\mathbf{x}) = \frac{1}{(2\pi)^d} \sum_{\mathbf{q} \in \mathcal{Q}_d} \theta(\mathbf{q}) e^{\iota\langle \mathbf{q}, \mathbf{x} \rangle}. \quad (36)$$

We let θ_* , $\theta_{*,s}$, and $\hat{\theta}_{\lambda,p,m,n,\alpha}$ respectively denote the Fourier transform of f_* , $f_{*,s}$, and $\hat{f}_{\lambda,p,m,n,\alpha}$.

The Fourier transforms of the observations are given by

$$\hat{Y}(\mathbf{q}) = \theta_*(\mathbf{q}) + \frac{\sigma}{\sqrt{n}} G(\mathbf{q}), \quad \hat{Y}_s(\mathbf{q}) = \theta_{*,s}(\mathbf{q}) + \frac{\sigma_s}{\sqrt{m}} G_s(\mathbf{q}), \quad (37)$$

where $G(\mathbf{q})$ and $G_s(\mathbf{q})$ are i.i.d. standard Gaussian. It then follows that

$$\hat{\boldsymbol{\theta}}_{m,n}(\alpha) = \arg \min_{\boldsymbol{\theta}} \left\{ (1-\alpha) \|\hat{\mathbf{Y}} - \boldsymbol{\theta}\|_2^2 + \alpha \|\hat{\mathbf{Y}}_s - \boldsymbol{\theta}\|_2^2 + \lambda \|\boldsymbol{\theta}\|_{p,2}^2 \right\}. \quad (38)$$

where we abuse the notation to define

$$\|\boldsymbol{\theta}\|_{p,2}^2 := \sum_{\mathbf{q} \in \mathcal{Q}_d} c_{p,\mathbf{q}} |\boldsymbol{\theta}(\mathbf{q})|^2. \quad (39)$$

with $c_{p,\mathbf{q}} := 1 + \|\mathbf{q}\|^{2r}$. Minimizing (38) we get

$$\hat{\boldsymbol{\theta}}_{m,n}(\mathbf{q}; \alpha) = \frac{1}{1 + \lambda c_{p,\mathbf{q}}} [(1-\alpha) \hat{\mathbf{Y}}(\mathbf{q}) + \alpha \hat{\mathbf{Y}}_s(\mathbf{q})]. \quad (40)$$

Taking the inverse Fourier transform and plugging it into the excess risk formula we get

$$\begin{aligned} R(\hat{f}_{m,n,\alpha}) &= \sum_{\mathbf{q} \in \mathcal{Q}_d} \frac{1}{(1 + \lambda c_{p,\mathbf{q}})^2} [\alpha(\boldsymbol{\theta}_{*,s} - \boldsymbol{\theta}_*)(\mathbf{q}) \\ &\quad + \lambda c_{p,\mathbf{q}} \boldsymbol{\theta}_*(\mathbf{q})]^2 + V_{n,m} \sum_{\mathbf{q} \in \mathcal{Q}_d} \frac{1}{(1 + \lambda c_{p,\mathbf{q}})^2}, \end{aligned} \quad (41)$$

where

$$V_{n,m} := (1-\alpha)^2 \frac{\sigma^2}{n} + \alpha^2 \frac{\sigma_s^2}{m}. \quad (42)$$

The convexity of $x \rightarrow x^2$ implies

$$(a+b)^2 = \left(\gamma \frac{a}{\gamma} + (1-\gamma) \frac{b}{1-\gamma} \right)^2 \leq \frac{a^2}{\gamma} + \frac{b^2}{1-\gamma} \quad (43)$$

for $\gamma \in (0, 1)$ and therefore we can upper bound the first sum in (41) by taking $\gamma = 1/(1+\delta)$ for any $\delta > 0$, which yields

$$R(f_{m,n,\alpha}) \leq (1+\delta) \alpha^2 \|\boldsymbol{\theta}_{*,s} - \boldsymbol{\theta}_*\|_2^2 + \frac{1+\delta}{\delta} \sum_{\mathbf{q} \in \mathcal{Q}_d} \left(\frac{\lambda c_{p,\mathbf{q}}}{1 + \lambda c_{p,\mathbf{q}}} \right)^2 |\boldsymbol{\theta}_*(\mathbf{q})|^2 + V_{n,m} \sum_{\mathbf{q} \in \mathcal{Q}_d} \frac{1}{(1 + \lambda c_{p,\mathbf{q}})^2}. \quad (44)$$

C.1 Proof of Theorem 1

We now upper bound the first sum above. We note that, defining q_0 via $\lambda c_r(q_0) = 1$ (with an abuse of notation $c_r(t) = 1 + t^{2r}$), whence $q_0 \geq (\lambda/2)^{-1/2r}$ for all $\lambda < 1$:

$$\begin{aligned} \sum_{\mathbf{q} \in \mathcal{Q}_d} \left(\frac{\lambda c_{p,\mathbf{q}}}{1 + \lambda c_{p,\mathbf{q}}} \right)^2 \cdot |\boldsymbol{\theta}_*(\mathbf{q})|^2 &\leq \sum_{\mathbf{q} \in \mathcal{Q}_d, \|\mathbf{q}\|_2 \leq q_0} \lambda^2 c_r(\mathbf{q})^2 |\boldsymbol{\theta}_*(\mathbf{q})|^2 + \sum_{\mathbf{q} \in \mathcal{Q}_d, \|\mathbf{q}\|_2 > q_0} |\boldsymbol{\theta}_*(\mathbf{q})|^2 \\ &\leq \lambda^2 \max_{\|\mathbf{q}\|_2 \leq q_0} \frac{c_r(\mathbf{q})^2}{c_s(\mathbf{q})} \sum_{\mathbf{q} \in \mathcal{Q}_d, \|\mathbf{q}\|_2 \leq q_0} c_s(\mathbf{q}) |\boldsymbol{\theta}_*(\mathbf{q})|^2 + \max_{\|\mathbf{q}\|_2 > q_0} \frac{1}{c_s(\mathbf{q})} \sum_{\mathbf{q} \in \mathcal{Q}_d, \|\mathbf{q}\|_2 > q_0} c_s(\mathbf{q}) |\boldsymbol{\theta}_*(\mathbf{q})|^2 \\ &\stackrel{(a)}{\leq} \lambda^2 \max_{\|\mathbf{q}\|_2 \leq q_0} \frac{c_r(\mathbf{q})^2}{c_s(\mathbf{q})} \max_{\|\mathbf{q}\|_2 > q_0} \frac{1}{c_s(\mathbf{q})} \end{aligned}$$

$$\begin{aligned}
&\leq \lambda^2 \max\left(1, \frac{c_r(q_0)^2}{c_s(q_0)}\right) + \frac{1}{c_s(q_0)} \\
&\leq C \max(\lambda^2, \lambda^{p/r}) + C\lambda^{p/r} \leq C\lambda^{2\wedge(p/r)},
\end{aligned}$$

where in (a) we used the fact that $\|f_*\|_{2,p}^2 = \sum_{\mathbf{q}} c_s(\mathbf{q})|\theta_*(\mathbf{q})|$. Letting $C_i(d)$ be constants depending on d , we have

$$\begin{aligned}
\sum_{\mathbf{q} \in \mathcal{Q}_d} \frac{1}{(1 + \lambda c_{r,\mathbf{q}})^2} &\leq C_1(d) \int_{\mathbb{R}^d} \frac{1}{(1 + \lambda c_{r,\mathbf{q}})^2} d\mathbf{q} \\
&\leq C_1(d) \int_{\mathbb{R}^d} \frac{1}{(1 + \lambda \|\mathbf{q}\|^{2r})^2} d\mathbf{q} \\
&\leq C_2(d) \int_0^\infty \frac{t^{d-1}}{(1 + \lambda t^{2r})^2} dt \\
&\leq C_2(d) \int_0^{\lambda^{-1/2r}} t^{d-1} dt + C_2(d) \lambda^{-2} \int_{\lambda^{-1/2r}}^\infty t^{d-1-4r} dt.
\end{aligned}$$

For convergence we require $r > d/4$, in which case

$$\sum_{\mathbf{q} \in \mathcal{Q}_d} \frac{1}{(1 + \lambda c_{r,\mathbf{q}})^2} \leq C_4(d) \lambda^{-d/2r}. \quad (45)$$

D Analysis of high-dimensional regression: Proofs for Section 5

D.1 Proof of Proposition 2

The proof is based on Gordon Gaussian comparison inequality [Gor85, Ver18], and follow a standard route, see e.g. [TOH15, TAH18, MM21]. We will limit ourselves to outlining the main steps of the calculation. Throughout, we consider the case $\varepsilon_0 > 0$, $\delta + \delta_s > 1$ because the other one ($\varepsilon_0 = 0$ and $\delta, \delta_s > 1$) is analogous and less interesting.

We begin by rewriting the ridge cost function in terms of a Lagrangian

$$\widehat{R}_{n,m}(\boldsymbol{\theta}; \alpha) = \max_{\mathbf{u} \in \mathbb{R}^n} \max_{\mathbf{u}^s \in \mathbb{R}^m} \widehat{L}_{n,m}(\boldsymbol{\theta}, \mathbf{u}, \mathbf{u}^s; \alpha), \quad (46)$$

$$\begin{aligned}
\widehat{L}_{n,m}(\boldsymbol{\theta}, \mathbf{u}, \mathbf{u}^s; \alpha) &:= \langle \mathbf{u}, \mathbf{X}(\boldsymbol{\theta} - \boldsymbol{\theta}_*) \rangle + \langle \mathbf{u}^s, \mathbf{X}^s(\boldsymbol{\theta} - \boldsymbol{\theta}_{*,s}) \rangle - \langle \mathbf{u}, \boldsymbol{\varepsilon} \rangle - \langle \mathbf{u}^s, \boldsymbol{\varepsilon}^s \rangle \\
&\quad - \frac{n\|\mathbf{u}\|_2^2}{2(1-\alpha)} - \frac{m\|\mathbf{u}^s\|_2^2}{2\alpha} + \frac{\lambda}{2} \|\boldsymbol{\theta}\|_2^2.
\end{aligned} \quad (47)$$

Let $\Delta(\boldsymbol{\theta}, \mathbf{u}, \mathbf{u}^s) := \|\mathbf{u}\|_2 \|\boldsymbol{\theta} - \boldsymbol{\theta}_*\|_2 G + \|\mathbf{u}^s\|_2 \|\boldsymbol{\theta} - \boldsymbol{\theta}_{*,s}\|_2 G_s$, where G, G_s are independent standard normal random variables, independent of \mathbf{X}, \mathbf{X}^s . By Gordon's inequality [Gor85], we can compare the Gaussian process $\widehat{L}_{n,m}(\boldsymbol{\theta}, \mathbf{u}, \mathbf{u}^s; \alpha) + \Delta(\boldsymbol{\theta}, \mathbf{u}, \mathbf{u}^s)$ to

$$\begin{aligned}
\widehat{L}_{n,m}^G(\boldsymbol{\theta}, \mathbf{u}, \mathbf{u}^s; \alpha) &:= \|\mathbf{u}\| \langle \mathbf{g}, \boldsymbol{\theta} - \boldsymbol{\theta}_* \rangle + \|\boldsymbol{\theta} - \boldsymbol{\theta}_*\| \langle \mathbf{h}, \mathbf{u} \rangle + \|\mathbf{u}^s\| \langle \mathbf{g}^s, \boldsymbol{\theta} - \boldsymbol{\theta}_{*,s} \rangle + \|\boldsymbol{\theta} - \boldsymbol{\theta}_{*,s}\| \langle \mathbf{h}, \mathbf{u}^s \rangle \\
&\quad - \langle \mathbf{u}, \boldsymbol{\varepsilon} \rangle - \langle \mathbf{u}^s, \boldsymbol{\varepsilon}^s \rangle - \frac{n\|\mathbf{u}\|_2^2}{2(1-\alpha)} - \frac{m\|\mathbf{u}^s\|_2^2}{2\alpha} + \frac{\lambda}{2} \|\boldsymbol{\theta}\|_2^2.
\end{aligned} \quad (48)$$

Next we define the orthonormal vectors

$$\mathbf{v}_* := \frac{\boldsymbol{\theta}_*}{\|\boldsymbol{\theta}_*\|_2}, \quad \mathbf{v}_*^\perp := \frac{\mathbf{P}_{\boldsymbol{\theta}_*}^\perp \boldsymbol{\theta}_{*,s}}{\|\mathbf{P}_{\boldsymbol{\theta}_*}^\perp \boldsymbol{\theta}_{*,s}\|_2}, \quad (49)$$

where $\mathbf{P}_{\boldsymbol{\theta}_*}^\perp = \mathbf{I} - \mathbf{P}_{\boldsymbol{\theta}_*} := \mathbf{I} - \mathbf{v}_* \mathbf{v}_*^\top$ is the projector orthogonal to $\boldsymbol{\theta}_*$. We then decompose

$$\boldsymbol{\theta} = \xi \mathbf{v}_* + \xi_\perp \mathbf{v}_*^\perp + \boldsymbol{\theta}^\perp, \quad (50)$$

where $\langle \mathbf{v}_*, \boldsymbol{\theta}^\perp \rangle = \langle \mathbf{v}_*^\perp, \boldsymbol{\theta}^\perp \rangle = 0$, and define $\omega := \|\boldsymbol{\theta}^\perp\|_2$. Defining $\tau^2 = \|\boldsymbol{\theta} - \boldsymbol{\theta}_*\|_2^2$, $\tau_s^2 = \|\boldsymbol{\theta} - \boldsymbol{\theta}_{*,s}\|_2^2$, Eq. (22) follows.

With these notations, and letting $\hat{\sigma}^2 = \|\tau \mathbf{h} + \boldsymbol{\varepsilon}\|_2^2/n - \tau^2$, $\hat{\sigma}_s^2 = \|\tau_s \mathbf{h}^s + \boldsymbol{\varepsilon}^s\|_2^2/m - \tau_s^2$, we get

$$\widehat{\mathcal{L}}_{n,m}^G(\boldsymbol{\theta}, \rho, \rho_s; \alpha) := \max_{\mathbf{u}, \mathbf{u}^s} \left\{ \widehat{L}_{n,m}^G(\boldsymbol{\theta}, \mathbf{u}, \mathbf{u}^s; \alpha) : \|\mathbf{u}\| = \frac{\rho}{\sqrt{d}}, \|\mathbf{u}^s\| = \frac{\rho_s}{\sqrt{d}} \right\}, \quad (51)$$

$$\begin{aligned} \widehat{\mathcal{L}}_{n,m}^G(\boldsymbol{\theta}, \rho, \rho_s; \alpha) &= \frac{\rho}{\sqrt{d}} \langle \mathbf{g}, \boldsymbol{\theta} - \boldsymbol{\theta}_* \rangle + \frac{\rho_s}{\sqrt{d}} \langle \mathbf{g}^s, \boldsymbol{\theta} - \boldsymbol{\theta}_{*,s} \rangle + \rho \sqrt{\delta(\tau^2 + \hat{\sigma}^2)} + \rho_s \sqrt{\delta_s(\tau_s^2 + \hat{\sigma}_s^2)} \\ &\quad - \frac{\delta \rho^2}{2(1-\alpha)} - \frac{\delta_s \rho_s^2}{2\alpha} + \frac{\lambda}{2} (\xi^2 + \xi_\perp^2 + \omega^2). \end{aligned} \quad (52)$$

We finally decompose $\mathbf{g} = \mathbf{g}_\parallel + \mathbf{g}_\perp$ where $\mathbf{g}_\parallel \in \text{span}(\mathbf{v}_*, \mathbf{v}_*^\perp)$ and $\mathbf{g}_\perp \perp \text{span}(\mathbf{v}_*, \mathbf{v}_*^\perp)$, and similarly for \mathbf{g}_s , and define

$$\mathcal{L}_{n,m}^G(\xi, \xi_\perp, \omega, \rho, \rho_s; \alpha) := \min_{\boldsymbol{\theta}} \left\{ \widehat{\mathcal{L}}_{n,m}^G(\boldsymbol{\theta}, \rho, \rho_s; \alpha) : \boldsymbol{\theta} = \xi \mathbf{v}_* + \xi_\perp \mathbf{v}_*^\perp + \boldsymbol{\theta}^\perp, \|\boldsymbol{\theta}^\perp\| = \omega \right\}. \quad (53)$$

Defining ι via $\|\rho \mathbf{g}_\perp / \sqrt{n} + \rho_s \mathbf{g}_{s,\perp} / \sqrt{m}\| = (1 + \iota) \sqrt{\rho^2 + \rho_s^2}$, we obtain

$$\begin{aligned} \mathcal{L}_{n,m}^G(\xi, \xi_\perp, \omega, \rho, \rho_s; \alpha) &= -(1 + \iota) \sqrt{\rho^2 + \rho_s^2} \cdot \omega + \Delta + \rho \sqrt{\delta(\tau^2 + \hat{\sigma}^2)} + \rho_s \sqrt{\delta_s(\tau_s^2 + \hat{\sigma}_s^2)} \\ &\quad - \frac{\delta \rho^2}{2(1-\alpha)} - \frac{\delta_s \rho_s^2}{2\alpha} + \frac{\lambda}{2} (\xi^2 + \xi_\perp^2 + \omega^2), \end{aligned} \quad (54)$$

where Δ is the contribution of the perpendicular components. Simple concentration estimates imply that for any $\varepsilon > 0$ there exist $c(\varepsilon) > 0$ such that

$$\mathbb{P}(|\hat{\sigma} - \sigma| \leq \varepsilon \sqrt{\tau^2 + \sigma^2}, |\hat{\sigma}_s - \sigma_s| \leq \varepsilon \sqrt{\tau_s^2 + \sigma_s^2}) \geq 1 - e^{-c(\varepsilon)n}, \quad (55)$$

$$\mathbb{P}(\Delta \leq \sqrt{(\rho^2 + \rho_s^2)(\xi^2 + \xi_\perp^2)}) \geq 1 - e^{-c(\varepsilon)n}, \quad (56)$$

$$\mathbb{P}(|\iota| \leq \varepsilon) \geq 1 - e^{-c(\varepsilon)n}. \quad (57)$$

We can then estimate $\mathcal{L}_{n,m}^G(\xi, \xi_\perp, \omega, \rho, \rho_s; \alpha)$ by

$$\begin{aligned} \mathcal{L}^G(\xi, \xi_\perp, \omega, \rho, \rho_s; \alpha) &= -\sqrt{\rho^2 + \rho_s^2} \cdot \omega + \rho \sqrt{\delta(\tau^2 + \sigma^2)} + \rho_s \sqrt{\delta_s(\tau_s^2 + \sigma_s^2)} \\ &\quad - \frac{\delta \rho^2}{2(1-\alpha)} - \frac{\delta_s \rho_s^2}{2\alpha} + \frac{\lambda}{2} (\xi^2 + \xi_\perp^2 + \omega^2), \end{aligned} \quad (58)$$

Differentiating with respect to ρ and ρ_s and setting the derivatives to 0 yields $\rho = \bar{\rho}/\sqrt{1+t^2}$, $\rho_s = \bar{\rho}t/\sqrt{1+t^2}$, with $\bar{\rho}, t$ given by Eqs. (23), (24). By computing second derivatives, one obtain that this is a local maximum. Since $\mathcal{L}^G(\xi, \xi_\perp, \omega, \rho, \rho_s; \alpha) \rightarrow -\infty$ as $\rho^2 + \rho_s^2 \rightarrow \infty$, the maximum over ρ, ρ_s is either achieved at this point or at the boundary $\{\rho = 0\} \cup \{\rho_s = 0\}$. By checking the signs of partial derivatives along this boundary, the only other possibility is $\rho = \rho_s = 0$.

For economy of notation, write $F(\rho, \rho_s) := \mathcal{L}^G(\xi, \xi_\perp, \omega, \rho, \rho_s; \alpha)$. For any unit vector $\mathbf{v} = (v_1, v_2) \geq 0$, the directional derivative is

$$\nabla_{\mathbf{v}} F(\mathbf{r}) \Big|_{\mathbf{r}=0} = -\omega + v_1 \sqrt{\delta(\tau^2 + \sigma^2)} + v_2 \sqrt{\delta_s(\tau_s^2 + \sigma_s^2)}$$

$$\geq \omega[-1 + v_1\sqrt{\delta} + v_2\sqrt{\delta_s}].$$

By maximizing over the direction, we see that \mathbf{v} can be chosen so that $\nabla_{\mathbf{v}}F(\mathbf{0}) \geq \omega[-1 + \sqrt{\delta + \delta_s}]$. Hence $\rho = \rho_s = 0$ cannot be the global aximum for $\delta + \delta_s > 1$.

Hence, we get

$$\mathcal{R}(\xi, \xi_{\perp}, \omega) = \max_{\rho, \rho_s \geq 0} \mathcal{L}^G(\xi, \xi_{\perp}, \omega, \rho, \rho_s; \alpha). \quad (59)$$

We further note that, for fixed $\rho, \rho_s > 0$, the function $(\xi, \xi_{\perp}, \omega) \mapsto \mathcal{L}^G(\xi, \xi_{\perp}, \omega, \rho, \rho_s; \alpha)$ is jointly strictly convex for $\lambda > 0$. Hence $(\xi, \xi_{\perp}, \omega) \mapsto \mathcal{R}(\xi, \xi_{\perp}, \omega)$ is also strictly convex for $\lambda > 0$. Therefore, it has a unique minimizer, which we denote by $(\xi^*, \xi_{\perp}^*, \omega^*)$. Proceeding as in [MM21], we obtain the following result.

Proposition D.1. *Under the assumptions of Proposition 2, for any $\varepsilon, \varepsilon_0 > 0$ there exists $c = c(\varepsilon, \varepsilon_0) > 0$ such that, if $\alpha \in [\varepsilon_0, 1 - \varepsilon_0]$ (letting $\mathbf{P}^{\perp} := \mathbf{I} - \mathbf{v}_* \mathbf{v}_*^{\top} - \mathbf{v}_*^{\perp} (\mathbf{v}_*^{\perp})^{\top}$)*

$$\mathbb{P}\left\{|\langle \mathbf{v}_*, \hat{\boldsymbol{\theta}}_{m,n} \rangle - \xi^*| \leq \varepsilon, |\langle \mathbf{v}_*^{\perp}, \hat{\boldsymbol{\theta}}_{m,n} \rangle - \xi_{\perp}^*| \leq \varepsilon, \|\mathbf{P}^{\perp} \hat{\boldsymbol{\theta}}_{m,n}\| - \omega^* \leq \varepsilon\right\} \geq 1 - 2e^{-cn}. \quad (60)$$

In particular, the last proposition implies (a weaker form of) Theorem 2 whereby the supremum is taken over a finite net. Namely for $\eta > 0$, we define

$$N(\varepsilon_0, \eta) := [\varepsilon_0, 1 - \varepsilon_0] \cap \eta\mathbb{Z}.$$

Recalling that, in the present case, $R(\hat{\boldsymbol{\theta}}) = \|\hat{\boldsymbol{\theta}} - \boldsymbol{\theta}\|_2^2$, we obtain (after adjusting the constant c) we have therefore:

$$\mathbb{P}\left(\max_{\alpha \in N(\varepsilon_0, \eta)} |R(\hat{\boldsymbol{\theta}}_{m,n}(\alpha)) - \mathcal{R}^*(\alpha)| \geq \varepsilon\right) \geq 1 - 2e^{-cn}. \quad (61)$$

Finally, let $\mathbf{X}_+ \in \mathbb{R}^{(m+n) \times d}$ be the matrix obtained by stacking \mathbf{X} and \mathbf{X}_s . Given constants C_1, C_2, C_3 , define the good event

$$\mathcal{G} := \left\{C_1 n \leq \lambda_{\min}(\mathbf{X}_+^{\top} \mathbf{X}_+) \leq \lambda_{\max}(\mathbf{X}_+^{\top} \mathbf{X}_+) \leq C_2 n; \|\mathbf{X}^{\top} \mathbf{y}\| \leq C_3 n, \|\mathbf{X}_s^{\top} \mathbf{y}_s\| \leq C_3 n\right\} / \quad (62)$$

By a standard bound on eigenvalues of Wishart matrices [Ver18], for $\delta + \delta_s > 1$, we can choose C_1, C_2, C_3 such that

$$\mathbb{P}(\mathcal{G}) \geq 1 - 2e^{-cn}. \quad (63)$$

Further on \mathcal{G} , $\boldsymbol{\theta}_{m,n}(\alpha)$ is bounded (in ℓ_2 norm, and Lipschitz continuous in α). As a consequence, for a sufficiently large constant L ,

$$\mathbb{P}\left(|R(\hat{\boldsymbol{\theta}}_{m,n}(\alpha_1)) - R(\hat{\boldsymbol{\theta}}_{m,n}(\alpha_2))| \leq L|\alpha_1 - \alpha_2| \forall \alpha_1, \alpha_2 \in [\varepsilon_0, 1 - \varepsilon_0]\right) \geq 1 - 2e^{-cn}. \quad (64)$$

The claim follows by using this estimate together with Eq. (61).